

# Ab Initio Effective One-Electron Potential Operators. I. Applications for Charge-Transfer Energy in Effective Fragment Potentials

Bartosz Błasiak,<sup>1, a)</sup> Joanna D. Bednarska,<sup>1</sup> Marta Chołuj,<sup>1</sup> and Wojciech Bartkowiak<sup>1</sup>

Department of Physical and Quantum Chemistry, Faculty of Chemistry, Wrocław University of Science and Technology, Wybrzeże Wyspińskiego 27, Wrocław 50-370, Poland

(Dated: 4 February 2020)

The concept of the effective one-electron potentials (OEP) has been useful for many decades in efficient description of electronic structure of chemical systems, especially extended molecular aggregates such as interacting molecules in condensed phases. Here, a general method for effective OEP-based elimination of electron repulsion integrals (ERI), that is tuned towards the fragment-based calculation methodologies such as the second generation of the effective fragment potentials (EFP2) method, is presented. Two general types of the OEP operator matrix elements are distinguished and treated either via the distributed multipole expansion or the extended density fitting schemes developed in this work. The OEP technique is then applied to address the problem of using incomplete EFP2 settings in many applications in interaction energy and molecular dynamics simulations due to relatively high computational cost of evaluating the charge transfer (CT) effects as compared to other effects. The alternative OEP-based CT energy model is proposed in the context of the intermolecular perturbation theory with Hartree-Fock non-interacting gas-phase reference wavefunctions, compatible with the EFP2 formulation. It is found that the computational cost can be reduced up to 20 times as compared to the CT energy method within the EFP2 scheme without compromising the accuracy for a wide range of weakly interacting neutral molecular complexes. Therefore, it is believed that the proposed model can be used within the EFP2 framework, making the CT energy term no longer the bottleneck in EFP2-based simulations of complex systems.

## I. INTRODUCTION

Charge transfer (CT) between molecules occurs when the net electronic populations of interacting molecules change which leads to an additional stabilization of a molecular aggregate.<sup>1,2</sup> Although CT processes can be relatively easily scrutinized based on the total amount of electronic charge transferred between interacting species,<sup>1</sup> evaluation of its contribution to the intermolecular interaction potential<sup>2</sup> is far from trivial due to its notably complex quantum mechanical (QM) origins even at the Hartree-Fock<sup>3</sup> (HF) approximation level,<sup>4,5</sup> and cannot be realized in terms of any classical nor semi-classical approach. In fact, CT does not naturally emerge in the symmetry adapted perturbation theory<sup>6</sup> (SAPT) due to technical aspects related with the use of finite basis set expansions in modern quantum chemistry calculations and avoiding the basis set superimposition error (BSSE). Stone and Misquitta showed that CT energy can be extracted from SAPT calculations by comparing the induction energies of fictional systems in which basis functions are centered either on the monomers only, or the entire interacting complex.<sup>7</sup> CT energy was formulated by Murrell et al.<sup>8</sup> in their perturbation theory in the region of small wavefunction overlap up to second order. However, all these theories are computationally too expensive to apply for efficient calculation of intermolecular forces in molecular dynamics because they involve calculation of the electron repulsion integrals (ERI's) and their four-in-

dex transformation to molecular orbital (MO) basis.<sup>5</sup>

The apparent difficulty in theoretically characterizing the CT energy in terms of the interacting molecular fragments is indeed a challenge in the development of modern force fields or *ab initio* fragmentation methods<sup>9</sup> for modeling structure and dynamics in condensed phases.<sup>10</sup> This needs to be contrasted with the Coulombic electrostatics, non-Coulombic repulsion (i.e., due to Pauli exclusion principle), dispersion and induction for instance, which to a certain extent can be well described by relatively simple and computationally inexpensive to evaluate mathematical models, i.e., the distributed multipole moments of charge densities,<sup>11–13</sup> the van der Waals repulsive and attractive potentials, as well as the polarizability models. Due to this reason, the CT effects are not explicitly included in most of molecular mechanics force field developed up to date.<sup>14</sup> There is only a few force fields which explicitly incorporate the CT effects in the condensed-phase simulations in *ab initio* manner,<sup>15</sup> such as the second generation of the Effective Fragment Potential (EFP2) method<sup>4,16–23</sup> or Sum of Interactions Between Fragments Ab initio Computed (SIBFA) method<sup>24,25</sup>, apart from performing full QM electronic structure simulations or non-force-field-based fragmentation techniques<sup>26,27</sup>. EFP2, that is one of the most commonly used force fields of this kind, was derived on the grounds of the first-principles at the HF level<sup>4,22,23,28–30</sup> and including the intermolecular dispersion effects by the response theory.<sup>31,32</sup> That is to say, the total intermolecular interaction potential is approximated as

$$E^{\text{EFP2}} \approx E^{\text{Coul}} + E^{\text{Ex-Rep}} + E^{\text{Ind}} + E^{\text{Disp}} + E^{\text{CT}}, \quad (1)$$

where  $E^{\text{Coul}}$  is the Coulombic interaction energy of

<sup>a)</sup>blasjak.bartosz@gmail.com; <https://www.polonez.pwr.edu.pl>

the unperturbed charge-density distributions of the monomers, treated by the distributed multipole approximation with damping to account for the charge-penetration effects,<sup>33</sup>  $E^{\text{Ex-Rep}}$  is the exchange-repulsion energy originating from the Pauli exclusion principle,<sup>28,29</sup> that could be roughly understood as the Heitler-London interaction energy<sup>34</sup> with  $E^{\text{Coul}}$  subtracted,  $E^{\text{Ind}}$  and  $E^{\text{Disp}}$  are the induction and dispersion energies obtained from the distributed polarizability approximation,<sup>30–32</sup> and finally  $E^{\text{CT}}$  is the CT energy,<sup>22,23</sup> the focus of this work.

Despite the considerable success of the EFP2 theory in accurately modeling the extended molecular systems like solutions<sup>19–21,35</sup> and recently even biomolecules<sup>36–39</sup> with the level of accuracy reaching in many cases<sup>16</sup> the Møller-Plesset perturbation theory<sup>40</sup>, evaluation of the CT energy in EFP2 model is still relatively costly for typical uses in the molecular dynamics simulations. It has been reported that the implementation of the EFP2 CT energy and gradient in GAMESS US computer program<sup>41</sup> with canonical molecular orbitals is on average 20–30 times more demanding than the other components, becoming a bottleneck of the evaluation of total interaction energy and gradients.<sup>16,22</sup> Recent advancement of Xu and Gordon<sup>23</sup> reduced the cost further by about 50% by minimizing the size of the virtual orbital space via the use of quasiamionic minimal-basis orbitals<sup>42</sup> (QUAMBO's). Unfortunately, even with this improvement, the CT term remains still the most time-consuming to evaluate from among all the EFP2 terms.

In effect, the CT energy component is often ignored in some applications.<sup>35,38,39,43–48</sup> In fact, EFP2 CT term is available only in the GAMESS US quantum chemistry program,<sup>41</sup> whereas it is neither supported in the official release of the recent LIBEFP library for linking quantum chemistry packages with the EFP2 functionalities,<sup>49</sup> nor in the Q-CHEM quantum chemistry program,<sup>50</sup> contrary to electrostatic, exchange-repulsion, induction and dispersion EFP2 terms.

The effect of CT on the interaction energy is known to be often non-negligible, especially in donor-acceptor systems such as H-bonded species and charged complexes,<sup>51,52</sup> although it highly depends on the theoretical approach being used, i.e., the choice of the reference wavefunctions. The approach adopted by the founders of EFP2 model is based on gas-phase reference (unperturbed) HF wavefunctions, which will be here broadly referred to as the CT/HF0 level of theory and the symbol ‘0’ denotes unperturbed wavefunctions. In this formulation, the CT energy can be understood as a part of the polarization energy that cannot be linked to dispersion and pure induction interactions. In technical words, mixing of virtual and occupied MO's, that are assigned according to certain criteria to different unperturbed wavefunctions, occurs unlike the pure induction and dispersion, in which such mixings are contained solely within one monomer.<sup>2</sup>

One of the main goals of this work, apart from developing more efficient model of the CT/HF0 energy that

is compatible with the EFP2 energetics, is to extend the one-electron effective potentials (here referred to as the OEP) technique widely used previously<sup>3,5,22,53–61</sup> to simplify the rigorous and costly quantum chemistry models of extended systems with a particular emphasis on solvation phenomena and molecular dynamics. The presented OEP technique of removing ERI's from the working equations follows the notion of the importance of one-electron densities in chemistry<sup>54,55</sup>, thus reducing the complicated summations involving ERI's to much shorter expressions involving only one-electron integrals (OEI's). Therefore, the OEP computational method is first presented in Section II. Next, in Section III, the new technique is used to derive an alternative formulation of the CT/HF0 energy compatible with the EFP2 method. Subsequently, after details of computations are discussed in Section IV, in Section V the validation of the OEP-based CT/HF0 model is presented and its performance in terms of accuracy and computational speed is compared against the EFP2 model. Finally, few concluding remarks and outlook of future work are given in Section VI.

## II. EFFECTIVE ONE-ELECTRON POTENTIAL OPERATORS

To establish the notation within the present work, the formalism of one-electron potential operators is given first. The one-electron Coulomb static effective potential  $v^{\text{eff}}(\mathbf{r})$  produced by a certain effective one-electron charge density distribution  $\rho^{\text{eff}}(\mathbf{r})$  is

$$v^{\text{eff}}(\mathbf{r}) = \int \frac{\rho^{\text{eff}}(\mathbf{r}')}{|\mathbf{r}' - \mathbf{r}|} d\mathbf{r}', \quad (2)$$

where  $\mathbf{r}$  is a spatial coordinate. For convenience, the total effective density can be split into nuclear and electronic contributions,

$$\rho^{\text{eff}}(\mathbf{r}) = \lambda \rho_{\text{nuc}}^{\text{eff}}(\mathbf{r}) + \rho_{\text{el}}^{\text{eff}}(\mathbf{r}), \quad (3)$$

where  $\lambda$  is a certain parameter and is assumed to be either 1 or 0 in this work. Formally, the electronic part can be expanded in terms of an effective bond order matrix, or one-particle density (OED), represented in a certain basis of orbitals,  $\phi(\mathbf{r})$ ,

$$\rho_{\text{el}}^{\text{eff}}(\mathbf{r}) = - \sum_{\alpha\beta} P_{\alpha\beta}^{\text{eff}} \phi_{\alpha}(\mathbf{r}) \phi_{\beta}^*(\mathbf{r}). \quad (4)$$

Based on that, the operator form of the effective potential can be written as

$$\hat{v}^{\text{eff}} = \lambda \hat{v}_{\text{nuc}} + \int d\mathbf{r} |\mathbf{r}\rangle v_{\text{el}}^{\text{eff}}(\mathbf{r}) \langle \mathbf{r}| \quad (5)$$

with the nuclear operator defined by

$$\hat{v}_{\text{nuc}} \equiv \sum_x^{\text{At}} \int d\mathbf{r} |\mathbf{r}\rangle \frac{Z_x}{|\mathbf{r} - \mathbf{r}_x|} \langle \mathbf{r}|. \quad (6)$$

and  $\langle \mathbf{r} | \alpha \rangle \equiv \varphi_\alpha(\mathbf{r})$ . The matrix element of the effective potential operator is therefore given by

$$\langle \alpha | \hat{v}^{\text{eff}} | \beta \rangle = \lambda \sum_x^{\text{At}} W_{\alpha\beta}^{(x)} - \sum_{\gamma\delta} \langle \alpha\beta | \gamma\delta \rangle P_{\gamma\delta}^{\text{eff}}, \quad (7)$$

where

$$W_{\alpha\beta}^{(x)} = Z_x \int \frac{\phi_\alpha^*(\mathbf{r}) \phi_\beta(\mathbf{r})}{|\mathbf{r} - \mathbf{r}_x|} d\mathbf{r}, \quad (8)$$

$Z_x$  is the atomic number of the  $x$ th atom, and the symbol ‘At’ denotes all atoms that contribute to the effective potential. In the above equation and throughout the work,

$$\langle \alpha | \mathcal{O}(1) | \beta \rangle \equiv \int \phi_\alpha^*(\mathbf{r}) \mathcal{O}(1) \phi_\beta(\mathbf{r}) d\mathbf{r} \quad (9)$$

for any one-electron operator  $\mathcal{O}(1)$  and the ERI is defined according to

$$\langle \alpha\beta | \gamma\delta \rangle \equiv \iint \frac{\phi_\alpha^*(\mathbf{r}_1) \phi_\beta(\mathbf{r}_1) \phi_\gamma^*(\mathbf{r}_2) \phi_\delta(\mathbf{r}_2)}{|\mathbf{r}_1 - \mathbf{r}_2|} d\mathbf{r}_1 d\mathbf{r}_2. \quad (10)$$

### A. Incorporating Electron Repulsion Integrals into Effective Potentials

Consider now an arbitrary functional  $\mathcal{F}$  that explicitly depends on the ERI’s. In this work, OEP’s are defined by the following transformation

$$\mathcal{F} [\langle ij | k^A l^A \rangle] = \langle i | \hat{v}_{kl}^A | j \rangle, \quad (11)$$

where  $\hat{v}_{kl}^A$  is the effective OEP operator given by Eq. (5) with the effective density  $\rho_{kl}^A(\mathbf{r}) \equiv \phi_k^A(\mathbf{r}) \phi_l^A(\mathbf{r})$ . The summations over  $k$  and  $l$  can be incorporated into the total effective OEP operator  $\hat{v}_{\text{eff}}^A$  to produce

$$\sum_{ij} \sum_{kl \in A} \mathcal{F} [\langle ij | k^A l^A \rangle] = \sum_{ij} \langle i | \hat{v}_{\text{eff}}^A | j \rangle. \quad (12)$$

Thus, the total computational effort is, in principle, reduced from the fourth-fold sum involving evaluation of ERI’s to the two-fold sums of cheaper OEI’s. It is also possible to generalize the above expression even further by summing over all possible functionals  $\mathcal{F}_t$

$$\sum_t \sum_{ij} \sum_{kl \in A} \mathcal{F}_t [\langle ij | k^A l^A \rangle] = \sum_{ij} \langle i | \hat{v}_{\text{eff}}^A | j \rangle. \quad (13)$$

The above design has the advantage that it opens the possibility to define first-principles effective fragments as long as the functionals  $\mathcal{F}_t$  are well defined, computable and can be approximately partitioned in between the interacting fragments.

Three unique classes of ERI’s can be recognized based on the basis function partitioning scheme within the system composed of two molecules (shall be  $A$  and  $B$  throughout the course of this work). They are as follows:

1. the Coulomb-like ERI’s of the type  $\langle AA | BB \rangle \rightarrow \langle \phi_{i \in A} \phi_{k \in A} | \phi_{j \in B} \phi_{l \in B} \rangle$ ,
2. the overlap-like ERI’s of the type  $\langle AA | AB \rangle \rightarrow \langle \phi_{i \in A} \phi_{k \in A} | \phi_{j \in A} \phi_{l \in B} \rangle$ , and
3. the exchange-like ERI’s of the type  $\langle AB | AB \rangle \rightarrow \langle \phi_{i \in A} \phi_{j \in B} | \phi_{k \in A} \phi_{l \in B} \rangle$ .

In contrast to the first two classes of ERI’s, exchange-like ERI’s cannot be incorporated into OEP’s. The Coulomb and overlap-like classes, which are listed in Table I, are usually approximated via expanding the OEP operator in distributed multipole (DMTP) expansion series, and integrating over one remaining electron coordinate,<sup>22</sup> i.e.,

$$\langle j | \hat{v}_{\text{eff}}^A | l \rangle \cong \left\langle j \left| \sum_{w \in A} \left\{ T_{we}^{(0)} \hat{q}_w - \mathbf{T}_{we}^{(1)} \cdot \hat{\mathbf{\mu}}_w + \frac{1}{3} \mathbf{T}_{we}^{(2)} : \hat{\Theta}_w - \dots \right\} \right| l \right\rangle_{\mathbf{r}_e}. \quad (14)$$

In the above equation,  $\hat{q}_{\text{eff}}^{(w)}$ ,  $\hat{\mathbf{\mu}}_{\text{eff}}^{(w)}$  and  $\hat{\Theta}_{\text{eff}}^{(w)}$  are the quantum operators of effective distributed monopole (charge), dipole moment and quadrupole moment, respectively, centered on the  $w$ th site at  $\mathbf{r}_w$ , whereas  $\mathbf{T}_{we}^{(d)}$  are the so called interaction tensors of rank  $d$  between  $\mathbf{r}_w$  and  $\mathbf{r}_e$ , with the latter being the electronic coordinate. Explicit forms of interaction tensors can be found elsewhere.<sup>62</sup> Note that  $|j\rangle$  and  $|l\rangle$  can belong to either molecule. In this way, ERI’s are no longer needed and the computational cost reduces appreciably. In this work, this method is however considered already too expensive for application in the CT/HF0 energy because evaluation of Eq. (14) requires calculation of electrostatic potential and electrostatic potential gradient(s) OEI’s. These kind of integrals are typically the most expensive when compared to other standard OEI’s such as overlap or kinetic energy integrals. Therefore, Coulomb and overlap-like OEP matrix elements will be treated via more approximate and less expensive approaches which are discussed next.

TABLE I. Types of matrix elements with OEP operators

Matrix element	Overlap-like	Coulomb-like
	$\langle i   \hat{v}_{\text{eff}}^A   j \rangle$	$\langle j   \hat{v}_{\text{eff}}^A   l \rangle$
Partitioning scheme	$i \in A, j \in B$	$j, l \in B$
ERI class	$\langle AA   AB \rangle$	$\langle AA   BB \rangle$
DF <sup>a</sup> /RI <sup>b</sup> Form	$\sum_{\xi \in A} v_{i\xi}^A S_{\xi j}^{AB}$	$\sum_{\xi \in A} S_{j\xi}^{BA} v_{\xi\xi}^A S_{\xi l}^{AB}$
DMTP <sup>c</sup> Form	—	$\rho_{jl}^B \odot \rho_{\text{eff}}^A$

<sup>a</sup> Density Fitting

<sup>b</sup> Resolution of Identity

<sup>c</sup> Distributed Multipole Expansion

## B. Semi-classical multipole expansion

Semi-classical multipole expansion is the most applicable in case of matrix elements of the type  $\langle j^B | \hat{v}_{\text{eff}}^A | l^B \rangle$  because it can be considered as a Coulombic interaction between  $\rho_{jl}^B$  and  $\rho_{\text{eff}}^A$ . These matrix elements require ERI's of type  $\langle AA | BB \rangle$  only. In general, given certain two effective one-electron density distributions, the associated effective Coulombic interaction energy can be estimated from the classical formula according to

$$E_{\text{eff}} = \iint \frac{\rho_{\text{eff}}^X(\mathbf{r}_1)\rho_{\text{eff}}^Y(\mathbf{r}_2)}{|\mathbf{r}_1 - \mathbf{r}_2|} d\mathbf{r}_1 d\mathbf{r}_2. \quad (15)$$

The above integral can be approximated by applying the DMTP expansion to both effective potential operators and dropping the  $\hat{\cdot}$  symbol in the multipole operators which leads to:<sup>2</sup>

$$E_{\text{eff}} \approx \rho_{\text{eff}}^X \odot \rho_{\text{eff}}^Y \equiv \sum_{u \in A} \sum_{w \in B} \left\{ T_{uw}^{(0)} q_{\text{eff}}^{(u)} q_{\text{eff}}^{(w)} - \mathbf{T}_{uw}^{(1)} \cdot [q_{\text{eff}}^{(u)} \boldsymbol{\mu}_{\text{eff}}^{(w)} - q_{\text{eff}}^{(w)} \boldsymbol{\mu}_{\text{eff}}^{(u)}] - \mathbf{T}_{uw}^{(2)} : \boldsymbol{\mu}_{\text{eff}}^{(u)} \otimes \boldsymbol{\mu}_{\text{eff}}^{(w)} \dots \right\} \quad (16)$$

The symbol ‘ $\odot$ ’ denotes the sum of all the tensor contractions performed over the DMTP's of molecule  $X$  and  $Y$  to yield the associated interaction energy. The choice of the distribution centres as well as the truncation order of the multipole expansion is crucial in compromising the accuracy and computational cost of the resulting expressions. There are many ways in which this can be achieved, e.g., through the distributed multipole analysis (DMA) of Stone and Alderton<sup>13,63</sup>, the cumulative atomic multipole moments (CAMM) of Sokalski and Poirier<sup>11</sup>, the localised distributed multipole expansion (LMTP) of Etchegaray, Lavery and Pullman<sup>12</sup> or other schemes based on fitting to electrostatic potential, such as ChelpG<sup>64</sup>.

## C. Extended Density Fitting of OEP's

Extended density fitting of OEP's, which will be referred to as the EDF scheme, is applicable in case of matrix elements of  $\langle i^A | \hat{v}_{\text{eff}}^A | j^B \rangle$  type. These matrix elements require ERI's of type  $\langle AA | AB \rangle$  only. To get the *ab initio* representation of such an overlap-like matrix element, one can use a procedure similar to the typical density fitting (DF) or resolution of identity (RI), which are nowadays widely used to compute electron-repulsion integrals (ERI's) more efficiently, and reduce computational cost of post-Hartree-Fock methods.<sup>65</sup> Density fitting was also applied to design *ab initio* force fields.<sup>58,59</sup>

## 1. Density Fitting in Nearly-Complete Space

An arbitrary one-electron potential of molecule  $A$  acting on any state vector associated with molecule  $A$  can be expanded in an auxiliary space centered on  $A$  as

$$\hat{v}^A |i\rangle = \sum_{\xi\eta}^{\text{RI}} \hat{v}^A |\xi\rangle [\mathbf{S}^{-1}]_{\xi\eta} \langle \eta | i \rangle \quad (17)$$

under the necessary assumption that the auxiliary basis set is nearly complete, i.e.,  $\sum_{\xi\eta}^{\text{RI}} |\xi\rangle [\mathbf{S}^{-1}]_{\xi\eta} \langle \eta | \cong 1$ . In the equations above, the ‘RI’ symbol denotes a certain auxiliary basis set that fulfills such resolution of identity. The above general expansion can be also obtained by utilizing the density fitting in the nearly-complete space,

$$\hat{v}^A |i\rangle = \sum_{\xi}^{\text{RI}} V_{i\xi}^A |\xi\rangle. \quad (18)$$

In the above equation, the matrix  $\mathbf{V}^A$  is the projection of the state vector  $\hat{v}^A |i\rangle$  onto the nearly-complete basis  $\{\varphi_{\xi}\}$ . Let  $Z_i[\mathbf{V}^A]$  be the least-squares objective function

$$Z_i[\mathbf{V}^A] = \int |\Xi_i(\mathbf{r})|^2 d\mathbf{r} \quad (19)$$

with the error density defined by

$$\Xi_i(\mathbf{r}) = v^A(\mathbf{r})\phi_i(\mathbf{r}) - \sum_{\xi}^{\text{RI}} V_{i\xi}^A \varphi_{\xi}(\mathbf{r}). \quad (20)$$

By requiring that

$$\frac{\partial Z_i[\mathbf{V}^A]}{\partial V_{i\mu}^A} = 0 \text{ for all } \mu \quad (21)$$

one finds the coefficients of the  $i$ th row of  $\mathbf{V}^A$  to be

$$V_{i\xi}^A = \sum_{\eta}^{\text{RI}} [\mathbf{S}^{-1}]_{\xi\eta} a_{\eta}^{(i)}, \quad (22)$$

where the auxiliary matrices are given by

$$a_{\eta}^{(i)} = \int \varphi_{\eta}^*(\mathbf{r}) \hat{v}^A \phi_i(\mathbf{r}) d\mathbf{r}, \quad (23a)$$

$$S_{\eta\xi} = \int \varphi_{\eta}^*(\mathbf{r}) \varphi_{\xi}(\mathbf{r}) d\mathbf{r}. \quad (23b)$$

The working formula for  $a_{\eta}^{(i)}$  can be found by applying potential form from Eq. (2) along with the spectral representation of the effective density from Eq. (4) which finally gives

$$a_{\eta}^{(i)} = \lambda \sum_x W_{\eta i}^{(x)} - \sum_{\alpha\beta} P_{\alpha\beta}^A \langle \alpha\beta | \eta i \rangle. \quad (24)$$

Since only one step is required to obtain the OEP matrix, the scheme will be abbreviated as EDF-1.

## 2. Density Fitting in Incomplete Space

Density fitting scheme from previous section has practical disadvantage of a nearly-complete basis set being usually very large (spanned by large amount of basis set vectors). Since most of basis sets used in quantum chemistry do not form a nearly complete set, it is beneficial to design a modified scheme in which it is possible to obtain the effective matrix elements of the OEP operator in an incomplete auxiliary space. This can be achieved by minimizing the following objective function<sup>58,59</sup>

$$Z_i[\mathbf{V}^A] = \iint \frac{\Xi_i^*(\mathbf{r}_1)\Xi_i(\mathbf{r}_2)}{|\mathbf{r}_1 - \mathbf{r}_2|} d\mathbf{r}_1 d\mathbf{r}_2 . \quad (25)$$

with the error density defined by

$$\Xi_i(\mathbf{r}) = v^A(\mathbf{r})\phi_i(\mathbf{r}) - \sum_{\xi}^{\text{DF}} V_{i\xi}^A \varphi_{\xi}(\mathbf{r}) . \quad (26)$$

where the symbol ‘DF’ denotes the generally incomplete auxiliary basis set. From the requirement given in Eq. (21) one obtains

$$V_{i\xi}^A = \sum_{\eta}^{\text{DF}} [\mathbf{R}^{-1}]_{\xi\eta} b_{\eta}^{(i)} , \quad (27)$$

where

$$b_{\eta}^{(i)} = \iint \frac{\varphi_{\eta}^*(\mathbf{r}_1)\hat{v}^A\phi_i(\mathbf{r}_2)}{|\mathbf{r}_1 - \mathbf{r}_2|} d\mathbf{r}_1 d\mathbf{r}_2 , \quad (28a)$$

$$R_{\eta\xi} = \iint \frac{\varphi_{\eta}^*(\mathbf{r}_1)\varphi_{\xi}(\mathbf{r}_2)}{|\mathbf{r}_1 - \mathbf{r}_2|} d\mathbf{r}_1 d\mathbf{r}_2 . \quad (28b)$$

Note that, while  $R_{\eta\xi}$  is a typical 2-center ERI that can be evaluated by standard means,<sup>66</sup>  $b_{\eta}^{(i)}$  matrix elements are not trivial to calculate because the OEP operator, which contains integration over an electron coordinate, is present inside the double integral. Therefore, the following triple integral,

$$b_{\eta}^{(i)} = \iiint \frac{\varphi_{\eta}^*(\mathbf{r}_1)\phi_i(\mathbf{r}_2)\rho^{\text{eff}}(\mathbf{r}_3)}{|\mathbf{r}_1 - \mathbf{r}_2||\mathbf{r}_3 - \mathbf{r}_2|} d\mathbf{r}_1 d\mathbf{r}_2 d\mathbf{r}_3 , \quad (29)$$

has to be computed. Obtaining all the necessary integrals of this kind directly by performing integrations of Eq. (29) is very costly even for medium sized molecules.<sup>67</sup> However, one can introduce the effective potential in order to eliminate one integration. This can be achieved by performing additional density fitting in a nearly complete intermediate basis<sup>67</sup>

$$\hat{v}^{\text{eff}}|i\rangle = \sum_{\varepsilon}^{\text{RI}} H_{i\varepsilon}|\varepsilon\rangle , \quad (30)$$

The working equation is therefore given by

$$b_{\eta}^{(i)} = \sum_{\varepsilon}^{\text{RI}} H_{i\varepsilon} R_{\varepsilon\eta} , \quad (31)$$

which can be easily evaluated by noting that  $H_{i\varepsilon}$  components are given by Eq. (18) — thus, the matrix elements of the OEP operator can be found by using Eq. (27). It is emphasized here that, as long as the state vector  $|i\rangle$ , OEP operator  $\hat{v}^A$ , and the auxiliary and intermediate basis sets depend solely on the unperturbed molecule  $A$ , the matrix elements  $V_{i\xi}^A$  can be calculated just once and stored as effective fragment parameters.

In contrast to the EDF-1 scheme, two density fitting steps are now required to obtain the OEP matrix. Thus, extended density fitting in incomplete basis will be referred to as the EDF-2 scheme. In the limiting case, when the auxiliary basis is the same as the intermediate basis, EDF-2 is equivalent to EDF-1. As the theory required to define OEP’s and their computational evaluation in the fragment-based formulation has been finally given in this Section, the application of the OEP technique of ERI elimination is further discussed for the evaluation of the CT/HF0 energy in the following sections.

## III. CHARGE TRANSFER INTERACTION ENERGY FOR FRAGMENT POTENTIALS

In the CT/HF0 treatments of bi-molecular complexes, the CT energy can be expressed as a sum of the energy stabilization due to CT from molecule  $A$  to  $B$  and vice versa, i.e.,

$$E^{\text{CT}} = E^{A \rightarrow B} + E^{B \rightarrow A} . \quad (32)$$

### A. EFP2 Model

Li, Gordon and Jensen used the expansion of the overlap density in Taylor series and found four different approximate theories for the CT energy.<sup>22</sup> The optimal theory, which was shown to well reproduce the CT/HF0 energies obtained by using the reduced variational space (RVS) analysis of Stevens and Fink<sup>68</sup>, reads as

$$E^{A \rightarrow B} \approx 2 \sum_{i \in A}^{\text{Occ}} \sum_{n \in B}^{\text{Vir}} \frac{|U_{in}^{A \rightarrow B}|^2}{\varepsilon_i - T_{nn}} , \quad (33)$$

where

$$|U_{in}^{A \rightarrow B}|^2 \approx \frac{u_{in}}{1 - \sum_{m \in A}^{\text{All}} S_{mn}^2} \left\{ u_{in} + \sum_{j \in B}^{\text{Occ}} S_{ij} \left( T_{nj} - \sum_{m \in A}^{\text{All}} S_{nm} T_{mj} \right) \right\} , \quad (34)$$

and

$$u_{in} \equiv U_{in}^{\text{EF},B} - \sum_{m \in A}^{\text{All}} U_{im}^{\text{EF},B} S_{mn} , \quad (35)$$

in which the summations extend over occupied (denoted by ‘Occ’), virtual (denoted by ‘Vir’) or both (denoted by ‘All’) canonical HF MO’s. The effective potential energy matrix elements are defined by

$$U_{in}^{EF,B} \equiv -\langle i|\hat{v}_{\text{tot}}^B|n\rangle, \quad (36)$$

and are evaluated by expanding the  $\hat{v}_{\text{tot}}^B$  operator in distributed multipoles according to Eq. (14). The apparent success of the EFP2 scheme is rooted in the dramatic simplifications of the *ab initio* expressions for interaction energy, in which the relatively costly ERI’s have been effectively removed from the working models while maintaining the required accuracy. That is, in the case of the CT/EFP2 energy component, the canonical orbital energies  $\varepsilon_i$  are constant parameters, whereas the overlap  $S_{nm}$ , kinetic energy  $T_{mn}$  and effective one-electron electrostatic potential  $U_{in}^{EF}$  matrix elements are all certain types of the one-electron integrals, orders of magnitude cheaper to evaluate than ERI’s. Unfortunately, due to extensive summations over virtual orbitals, evaluating Eq. (33) is still considerable in cost because typically large basis sets need to be used for generating the EFP2 parameters. In effect, calculation of  $U_{in}^{EF}$  is much more expensive as compared to other types of one-electron integrals and is the bottleneck of CT/EFP2 energy calculation, even when using minimal amount of virtual orbitals.<sup>23</sup>

In the following subsections, the alternative model of the CT/HF0 energy is proposed by introducing OEP’s. Although application of the OEP method to the CT/HF0 formulation in EFP2 method is probably possible, it would be relatively difficult to discuss the resulting OEP-based EFP2 models because there are four distinct versions of this theory with a set of different approximations, selected based on performance assessment rather than a rigorous derivation manner.<sup>22</sup> Instead, perturbation theory of Murrell et al.<sup>8</sup> with the explicit formulation for closed shell systems by Otto and Ladik<sup>5</sup>, which is somewhat more rigorous than the EFP2 CT model, is chosen as a starting point in this work. It is believed that this choice will enable a clear demonstration of the OEP technique in fragment-based modelling.

## B. Otto-Ladik’s Model: Starting Point

The CT/HF0 energy can be expressed by<sup>5,8</sup>

$$E^{A \rightarrow B} = 2 \sum_{i \in A}^{\text{Occ}} \sum_{n \in B}^{\text{Vir}} \frac{|U_{in}^{A \rightarrow B}|^2}{\varepsilon_i - \varepsilon_n}, \quad (37)$$

where the coupling constant is given by Otto and Ladik,<sup>5</sup> here referred to as the OL method, as

$$\begin{aligned} U_{in}^{A \rightarrow B} = & -\langle i|\hat{v}_{\text{tot}}^B|n\rangle - \sum_{j \in B}^{\text{Occ}} \langle nj|ij\rangle \\ & + \sum_{k \in A}^{\text{Occ}} S_{nk} \langle k|\hat{v}_{\text{tot}}^B|i\rangle + \sum_{j \in B}^{\text{Occ}} S_{ij} \langle j|\hat{v}_i^A|n\rangle \\ & + \sum_{k \in A}^{\text{Occ}} \sum_{j \in B}^{\text{Occ}} S_{kj} (1 + \delta_{ik}) \langle nj|ik\rangle. \end{aligned} \quad (38)$$

In the above expression, the following effective one-electron potential operators,

$$\hat{v}_{\text{tot}}^B = \hat{v}_{\text{nuc}}^B + 2 \sum_{j \in B}^{\text{Occ}} \hat{v}_{jj}^B \quad \text{and} \quad (39a)$$

$$\hat{v}_i^A = \hat{v}_{\text{tot}}^A - 2\hat{v}_{ii}^A, \quad (39b)$$

were introduced without making any approximation to the original equation from Ref.<sup>5</sup> Note that ERI’s in MO basis are necessary to evaluate all terms in Eq. (38), e.g.,  $\langle i|\hat{v}_{\text{tot}}^B|n\rangle \equiv W_{nj}^B - 2 \sum_{j \in B} \langle in|jj\rangle$ . Therefore, the goal of this work is to apply the technique sketched in Eq. (13) to effectively eliminate ERI’s from Eq. (38) in terms of OEP’s.

## C. Otto-Ladik’s Model: Application of OEP Technique

One can immediately notice that the five summation terms from Eq. (38) can be classified based on Table I into three groups regarding the type of ERI’s that are required: (i) overlap-like  $\langle AB|BB\rangle$  – the first two terms; (ii) Coulomb-like  $\langle AA|BB\rangle$  – the third term and (iii) Coulomb-like  $\langle BB|AA\rangle$  – the two last terms. Note also that there are no exchange-like terms needed in this case. Therefore, all the contributions can be re-cast in terms of the OEP’s.

a. *Group (i).* Group (i) can be rewritten by noticing that

$$\sum_{j \in B}^{\text{Occ}} \langle nj|ij\rangle = \langle i|[-\hat{v}_{nj}^B|j\rangle], \quad (40)$$

which, by combining with the first term from Eq. (38), allows to apply the two-step extended density fitting (EDF-2) developed in Section II C 2 as follows

$$\langle i| \left[ -\hat{v}_{\text{tot}}^B|n\rangle + \sum_{j \in B}^{\text{Occ}} \hat{v}_{nj}^B|j\rangle \right] \cong \langle i| \sum_{\eta \in B}^{\text{DF}} V_{n\eta}^B|\eta\rangle \quad (41)$$

with the error density given by

$$\Xi_n(\mathbf{r}) = \left\{ v_{nuc}^B(\mathbf{r}) + 2 \sum_{j \in B}^{\text{Occ}} \int \frac{|\phi_j(\mathbf{r}')|^2}{|\mathbf{r}' - \mathbf{r}|} d\mathbf{r}' \right\} \phi_n(\mathbf{r}) - \sum_{j \in B}^{\text{Occ}} \phi_j(\mathbf{r}) \int \frac{\phi_n^*(\mathbf{r}') \phi_j(\mathbf{r}')}{|\mathbf{r}' - \mathbf{r}|} d\mathbf{r}' - \sum_{\eta \in B}^{\text{DF}} V_{n\eta}^B \varphi_\eta(\mathbf{r}) . \quad (42)$$

Substituting the above equation into Eq. (25) leads to

$$V_{n\xi}^B = \sum_{\eta \in B}^{\text{DF}} [\mathbf{R}^{-1}]_{\xi\eta} b_\eta^{(n)} , \quad (43)$$

where

$$b_\eta^{(n)} = \iint d\mathbf{r}_1 d\mathbf{r}_2 \frac{\varphi_\eta^*(\mathbf{r}_1)}{|\mathbf{r}_1 - \mathbf{r}_2|} \times \left[ \hat{v}_{\text{tot}}^B \phi_n(\mathbf{r}_2) - \sum_{j \in B}^{\text{Occ}} \hat{v}_{nj}^B \phi_j(\mathbf{r}_2) \right] . \quad (44)$$

The above result is given by a sum of triple integrals from Eq. (29). However, the following application of the resolution of identity,

$$- \hat{v}_{\text{tot}}^B |n\rangle + \sum_{j \in B}^{\text{Occ}} \hat{v}_{nj}^B |j\rangle \cong \sum_{\varepsilon \in B}^{\text{RI}} H_{n\varepsilon}^B |\varepsilon\rangle , \quad (45)$$

leads to a much simpler formula that requires only OEI's and ERI's. Therefore, by combining equations (43), (31) and (22) one arrives to

$$V_{n\xi}^B = \sum_{\eta \in B}^{\text{DF}} \sum_{\varepsilon \in B}^{\text{RI}} [\mathbf{R}^{-1}]_{\xi\eta} R_{\eta\varepsilon} H_{n\varepsilon}^B , \quad (46)$$

where

$$H_{n\varepsilon}^B = \sum_{\zeta \in B}^{\text{RI}} [\mathbf{S}^{-1}]_{\varepsilon\zeta} a_\zeta^{(n)} \quad (47)$$

and

$$\begin{aligned} a_\zeta^{(n)} &= -\langle \zeta | \hat{v}_{\text{tot}}^B | n \rangle + \sum_{j \in B}^{\text{Occ}} \langle \zeta | \hat{v}_{nj}^B | j \rangle \\ &= -\sum_{y \in B} W_{\zeta n}^{(y)} + \sum_{j \in B}^{\text{Occ}} \{ 2\langle \zeta n | jj \rangle - \langle \zeta j | nj \rangle \} . \end{aligned} \quad (48)$$

Note that all the calculations that are required to obtain  $V_{n\xi}^B$  are performed solely on the densities and basis sets associated with the unperturbed molecule  $B$ . Therefore,  $V_{n\xi}^B$  can be considered as effective fragment parameters used to compute the first two terms of Eq. (38) by

$$- \langle i | \hat{v}_{\text{tot}}^B | n \rangle - \sum_{j \in B}^{\text{Occ}} \langle nj | ij \rangle = \sum_{\eta \in B}^{\text{RI}} V_{n\eta}^B S_{\eta i} , \quad (49)$$

which is a great simplification over the original form of group (i) because only the overlap integrals between the  $i$ th MO on molecule  $A$  and  $\eta$ th auxiliary orbital on molecule  $B$  need to be evaluated. Note that the only approximation made so far was the application of density fitting and resolution of identity. If the auxiliary and intermediate basis sets are sufficiently large, the errors due to this approximation can be minimal and negligible in principle.

*b. Group (ii).* The term belonging to this group can be considered as a sum of interaction energies between the total charge density distribution of molecule  $B$  and the partial density  $\rho_{ik}(\mathbf{r})$  of molecule  $A$ , weighted by the overlap integrals  $S_{nk}$ . Using the distributed multipole expansion based on the charge centroids of the localized molecular orbitals (LMO's),  $\mathbf{r}_i = \langle i | \hat{\mathbf{r}} | i \rangle$  with  $\chi_i(\mathbf{r})$  being localized, this group can be approximated by

$$\sum_{k \in A}^{\text{Occ}} S_{nk} \langle k | \hat{v}_{\text{tot}}^B | i \rangle \approx S_{ni} \rho_{ii}^A \odot \rho_{\text{tot}}^B . \quad (50)$$

Here, it was assumed that  $|\rho_{ik}(\mathbf{r})| \ll \rho_{ii}(\mathbf{r})$  for  $i \neq k$  in most locations in the case of LMO's, which allows one to conjecture that

$$\rho_{ki}^A \odot \rho_{\text{tot}}^B \approx \delta_{ik} \rho_{ii}^A \odot \rho_{\text{tot}}^B . \quad (51)$$

Now, the DMTP expansion of the interaction energy in the right hand side of Eq. (51) can be given by

$$\rho_{ii}^A \odot \rho_{\text{tot}}^B \approx q_i \left[ \sum_{y \in B}^{\text{At}} \frac{Z_y}{|\mathbf{r}_y - \mathbf{r}_i|} + 2 \sum_{j \in B}^{\text{Occ}} \frac{q_j}{|\mathbf{r}_j - \mathbf{r}_i|} \right] , \quad (52)$$

because the distributed charges  $q_i = -1$  whereas the distributed dipole moments centered at their respective LMO charge centroids vanish.<sup>12</sup> This means that Eq. (50) can be finally given as follows:

$$\sum_{k \in A}^{\text{Occ}} S_{nk} \langle k | \hat{v}_{\text{tot}}^B | i \rangle \approx -S_{ni} \left[ \sum_{y \in B}^{\text{At}} \frac{Z_y}{r_{yi}} - \sum_{j \in B}^{\text{Occ}} \frac{2}{r_{ji}} \right] . \quad (53)$$

Therefore, only overlap integrals and relative distances between atomic and LMO centroid positions are needed, which leads to a great reduction of the calculation cost, as compared either to the original expression or to the multipole expansion (left- and right-hand sides of Eq. (50), respectively). We shall refer to this approximation as to the localized overlap approximation (LOA) resulting in similar expressions to the ones obtained by Jensen and Gordon in their exchange-repulsion interaction energy EFP2 model (see Eq. (39) in Ref.<sup>28</sup>). Note that, to make this approximation valid, occupied molecular orbitals need to be spatially localized.

*c. Group (iii).* The terms with the overlap integrals involving the occupied MO on  $A$  can be combined into a

single summation term, i.e.,

$$\begin{aligned}
& \sum_{j \in B}^{\text{Occ}} S_{ij} \langle j | \hat{v}_i^A | n \rangle + \sum_{k \in A}^{\text{Occ}} \sum_{j \in B}^{\text{Occ}} S_{kj} (1 - \delta_{ik}) \langle nj | ik \rangle \\
&= \sum_{k \in A}^{\text{Occ}} \sum_{j \in B}^{\text{Occ}} S_{kj} \langle j | \underbrace{\{ \delta_{ik} (\hat{v}_k^A + \hat{v}_{ik}^A) - \hat{v}_{ik}^A \}}_{\hat{v}_{ik}^{A,\text{eff}}} | n \rangle \\
&\cong \sum_{k \in A}^{\text{Occ}} \sum_{j \in B}^{\text{Occ}} S_{kj} \rho_{nj}^B \odot \rho_{ik}^{A,\text{eff}} , \quad (54)
\end{aligned}$$

where the effective potential  $v_{ik}^{A,\text{eff}}$  (with the associated effective density  $\rho_{ik}^{A,\text{eff}}$ ) is defined by

$$v_{ik}^{A,\text{eff}}(\mathbf{r}) \equiv \delta_{ik} [v_{\text{tot}}^A(\mathbf{r}) - 2v_{kk}^A(\mathbf{r}) + v_{ik}^A(\mathbf{r})] - v_{ik}^A(\mathbf{r}) . \quad (55)$$

In order to include the  $\rho_{nj}^B$  density, it is approximately represented here by a set of effective cumulative atomic charges  $\{q_y^{B,(nj)}\}$  associated with the effective one-particle density matrix

$$P_{\beta\delta}^{B,(nj)} = C_{\beta n} C_{\delta j} . \quad (56)$$

In this work, the effective charges were defined via the Mulliken method as discussed in Appendix B1 with  $\lambda = 0$ . By applying the LOA in LMO picture for the  $\rho_{ik}^A$  density the effective potential from Eq. (55) simplifies to

$$v_{ik}^{A,\text{eff}}(\mathbf{r}) \approx \delta_{ik} \{v_{\text{tot}}^A(\mathbf{r}) - 2v_{kk}^A(\mathbf{r})\} , \quad (57)$$

which leads to

$$\begin{aligned}
& \sum_{j \in B}^{\text{Occ}} S_{ij} \langle j | \hat{v}_{\text{tot}}^A | n \rangle + \sum_{k \in A}^{\text{Occ}} \sum_{j \in B}^{\text{Occ}} S_{kj} \langle nj | ik \rangle \\
& \approx \sum_{j \in B}^{\text{Occ}} S_{ij} \sum_{y \in B}^{\text{At}} q_y^{B,(nj)} \left[ \sum_{x \in A}^{\text{At}} \frac{Z_x}{r_{xy}} + \frac{2}{r_{iy}} - \sum_{k \in A}^{\text{Occ}} \frac{2}{r_{ky}} \right] . \quad (58)
\end{aligned}$$

*d. Final OEP-based forms of the coupling constant.* Gathering the results from Eqs. (49), (53) and (58) the coupling constant can be given as follows

$$U_{in}^{A \rightarrow B} \approx G_{1;in}^{A \rightarrow B} + G_{2;in}^{A \rightarrow B} + G_{3;in}^{A \rightarrow B} , \quad (59)$$

where

$$G_{1;in}^{A \rightarrow B} \equiv \sum_{\eta \in B}^{\text{RI}} V_{n\eta}^B S_{\eta i} , \quad (60a)$$

$$G_{2;in}^{A \rightarrow B} \equiv -S_{ni} u_i^{BA} , \quad (60b)$$

$$G_{3;in}^{A \rightarrow B} \equiv \sum_{j \in B}^{\text{Occ}} S_{ij} \sum_{y \in B}^{\text{At}} q_y^{B,(nj)} w_{yi}^{BA} . \quad (60c)$$

In the above, the auxiliary variables are

$$u_i^{BA} \equiv \sum_{y \in B}^{\text{At}} \frac{Z_y}{r_{yi}} - \sum_{j \in B}^{\text{Occ}} \frac{2}{r_{ji}} , \quad (61a)$$

$$w_{yi}^{BA} \equiv \sum_{x \in A}^{\text{At}} \frac{Z_x}{r_{xy}} + \frac{2}{r_{iy}} - \sum_{k \in A}^{\text{Occ}} \frac{2}{r_{ky}} . \quad (61b)$$

To compute the interaction energy due to CT from  $A$  to  $B$  by using the above LOA-based approximations, coupling elements need to be transformed from localized to canonical MO basis, i.e.,

$$E^{A \rightarrow B} \approx 2 \sum_{i \in A}^{\text{CMO}} \sum_{n \in B}^{\text{Vir}} \frac{|\sum_{i' \in A}^{\text{LMO}} L_{ii'}^A U_{i'n}^{A \rightarrow B}|^2}{\varepsilon_i - \varepsilon_n} , \quad (62)$$

where  $\mathbf{L}^A$  is the CMO-LMO transformation matrix for occupied orbitals of  $A$ . Note however, that the effective potential parameters from the density fitted term of group (i) do not involve any occupied orbitals. Therefore, to save computational costs, only groups (ii) and (iii) need to be transformed whereas for group (i) the overlap integrals from Eq. (49) can be already evaluated in CMO basis. This leads to the coupling constant of the following form,

$$V_{in}^{A \rightarrow B} \approx G_{1,in}^{A \rightarrow B} + \sum_{i' \in A}^{\text{LMO}} L_{ii'}^A \{G_{2,i'n}^{A \rightarrow B} + G_{3,i'n}^{A \rightarrow B}\} , \quad (63)$$

where the subscripts  $G_n$  ( $n = 1, 2, 3$ ) denote a particular group of terms from Eqs. (49), (53) and (58). Thus, the final working formula for the interaction energy due to CT from  $A$  to  $B$  reads as

$$\begin{aligned}
E^{A \rightarrow B} \approx & 2 \sum_{i \in A}^{\text{CMO}} \sum_{n \in B}^{\text{Vir}} \frac{1}{\varepsilon_i - \varepsilon_n} \times \left( G_{1,in}^{A \rightarrow B} \right. \\
& \left. + \sum_{i' \in A}^{\text{LMO}} L_{ii'}^A \{G_{2,i'n}^{A \rightarrow B} + G_{3,i'n}^{A \rightarrow B}\} \right)^2 . \quad (64)
\end{aligned}$$

The total CT energy is given by the sum of the above contribution and the twin contribution due to CT from molecule  $B$  to  $A$  according to Eq. (32).

#### IV. CALCULATION DETAILS

Four complexes: (i)  $(\text{H}_2\text{O})_2$ , (ii)  $\text{H}_2\text{O}-\text{CH}_3\text{OH}$ , (iii)  $\text{H}_2\text{O}-\text{NH}_4^+$  and (iv)  $\text{NO}_3^--\text{NH}_4^+$ , were chosen as model systems to analyse the asymptotic dependence of CT/HF0 energy. The reference (zero-displacement) geometries were obtained by performing energy-optimizations at the HF/6-31+G(d,p) level, as implemented in the GAUSSIAN16 quantum chemistry program package.<sup>69</sup> Subsequently, 30 displaced geometries for each model complex were obtained by translating one of the

monomers along the vector co-linear with the H-bond or N–N distance in the case of ammonium nitrate. The reference structures as well as the translation vectors are indicated in the insets of Figure 1 and S1. To perform statistical error analysis, structural databases of bi-molecular complexes in the non-covalent interactions database NCB31 developed by the Truhlar’s group,<sup>70–72</sup> as well as the BioFragment Database subset BBI for backbone-backbone interactions in proteins,<sup>73</sup> as implemented in the Psi4 program,<sup>74</sup> were utilized. In particular, the subsets from the NCB31 database were separately considered: the HB6/04 hydrogen bonding database,<sup>70–72</sup> the DI6/04 dipole interaction database,<sup>70–72</sup> the CT7/04 charge-transfer complex database,<sup>70–72</sup> the WI7/05 weak interaction database,<sup>70,72,75</sup> and the PPS5/05  $\pi$ - $\pi$  stacking database.<sup>70,72,75</sup>

The benchmark CT/HF0 energy was estimated from the following assumption:

$$E_{\text{HF0}}^{\text{CT}} \cong E_{\text{DDS/HF}}^{\text{Pol}} - E^{\text{Ind}}, \quad (65)$$

where  $E_{\text{DDS/HF}}^{\text{Pol}}$  is the Hartree-Fock polarization energy defined according to the density decomposition scheme (here referred as to the DDS) developed by Mandado and Hermida-Ramón,<sup>76</sup> whereas  $E^{\text{Ind}}$  term is the approximate pure induction energy due to the polarizability effects.<sup>2</sup> The DDS polarization energy encompasses all the charge delocalization effects that are not associated with the Pauli exclusion principle in the first order, and is computed by

$$E_{\text{DDS/HF}}^{\text{Pol}} \equiv \Delta E^{\text{HF}} - \left( E_{\text{DDS/HF}}^{\text{Coul}} + E_{\text{DDS/HF}}^{\text{Exch}} + E_{\text{DDS/HF}}^{\text{Rep}} \right). \quad (66)$$

In the above,  $\Delta E^{\text{HF}}$  is the total HF interaction energy,  $E_{\text{DDS/HF}}^{\text{Coul}}$  is the pure Coulombic interaction energy between the unperturbed (non-interacting) charge densities of the monomers in the complex, and  $E_{\text{DDS/HF}}^{\text{Exch}}$  and  $E_{\text{DDS/HF}}^{\text{Rep}}$  are the exchange and the Pauli-repulsion interaction energies, respectively. At the HF level of theory, the sum of the latter two terms, i.e., the exchange-repulsion energy,  $E_{\text{DDS/HF}}^{\text{Ex-Rep}}$ , is in fact equivalent to the exchange-repulsion energy in the intermolecular perturbation theory with exchange of Hayes and Stone.<sup>77</sup> It was also shown by Mandado and Hermida-Ramón,<sup>76</sup> that the Coulombic and exchange-repulsion term in the DDS method reproduce the first-order Coulombic and exchange-repulsion interaction energy in SAPT<sup>6</sup> with accuracy below 0.3 kcal/mole. Therefore, Eq. (65) is believed to be sufficient for evaluating the CT/HF0 energy, because there is no dispersion contribution to the DDS polarization energy at the HF level.

The pure induction energy was estimated by using the distributed dipole-dipole polarizability approximation according to the computational methodology of Li et al.,<sup>30</sup> in which

$$E^{\text{Ind}} \approx -\frac{1}{2} \mathbf{F}^{\text{T}} \cdot \Delta^{-1} \cdot \mathbf{F}. \quad (67)$$

In the above equation,  $\mathbf{F} = \{\dots, \mathbf{F}(\mathbf{r}_a), \dots\}$  is a super-vector of electric fields at the  $a$ th distributed site due to the surrounding unperturbed molecular charge densities in the complex (i.e., the charge-density of the molecule that contains  $a$ th center is not included in  $\mathbf{F}(\mathbf{r}_a)$ ). The matrix elements of  $\Delta$  are defined as

$$\Delta_{ab} = \begin{cases} \alpha_a^{-1} & \text{if } a = b \\ 0 & \text{if } a \neq b \wedge a, b \in \text{same molecule} \\ -\mathbf{T}_{ab} & \text{if } a \neq b \wedge a, b \notin \text{same molecule} \end{cases} \quad (68)$$

and  $\mathbf{T}_{ab}$  is the dipole-dipole interaction tensor given by

$$\mathbf{T}_{ab} \equiv \frac{3}{r_{ab}^5} \mathbf{r}_{ab} \otimes \mathbf{r}_{ab} - \frac{1}{r_{ab}^3} \mathbf{1}, \quad (69)$$

with  $\mathbf{r}_{ab} \equiv \mathbf{r}_a - \mathbf{r}_b$  being the relative distance between the LMO centroids. The electric fields at the LMO centroids were computed from the unperturbed HF charge-density distributions

$$\mathbf{F}(\mathbf{r}_a) = \sum_x^{\text{At}} \frac{Z_x}{r_{ax}^3} \mathbf{r}_{ax} + 2 \sum_{\alpha\gamma}^{\text{AO}} D_{\alpha\gamma} \left\langle \gamma \left| \frac{\mathbf{r}_a - \mathbf{r}}{|\mathbf{r}_a - \mathbf{r}|^3} \right| \alpha \right\rangle_{\mathbf{r}}, \quad (70)$$

in which  $\mathbf{D}$  is the one-particle density matrix. The distributed anisotropic dipole-dipole polarizabilities  $\alpha_a$  centered at the LMO centroids were computed by utilizing the coupled-perturbed Hartree-Fock method.<sup>78,79</sup> It was found here that accuracy of the LOA from Eqs. (53) and (58) is usually slightly better when the Boys method<sup>80</sup> is used, as compared to the Pipek-Mezey method<sup>81</sup>. Henceforth, the former method was used for molecular orbital localization throughout all the production calculations.

All the models that were used to test the theory presented in this work, i.e., the OL, EFP2 and OEP methods, as well as the EDF and the benchmark CT/HF0 and DDS methods, were implemented in our in-house plugin to Psi4 quantum chemistry program.<sup>74</sup> DDS method was implemented in the dimer-centered basis set<sup>34</sup> in order to eliminate the BSSE and properly include the CT processes.<sup>7</sup> Estimations of the  $E_{\text{DDS/HF}}^{\text{Coul}}$ ,  $E_{\text{DDS/HF}}^{\text{Ex-Rep}}$ ,  $E^{\text{Ind}}$  and  $E_{\text{EFP2}}^{\text{CT}}$  interaction energy components obtained by using the computer code developed for this work were found to be equivalent with the EFP2 interaction energy components obtained by using the GAMESS US package<sup>41</sup> (see Supplementary Information, Figure S2). For the CT EFP2 component, potential energy integrals from Eq. (14) were calculated with the CAMM up to quadrupoles (distributed centers are atoms), instead of the DMA (distributed centers are atoms and mid-bond points) as implemented in most of quantum chemistry programs. The choice of CAMM versus DMA was due to convenience of implementation and, because the quantitative accuracy of our EFP2 CT energy code is comparable to the EFP2 code of GAMESS US, using only atomic distribution centers does not affect the interpretation of results in Section V.

## V. RESULTS AND DISCUSSION

### A. Accuracy of OEP-based model

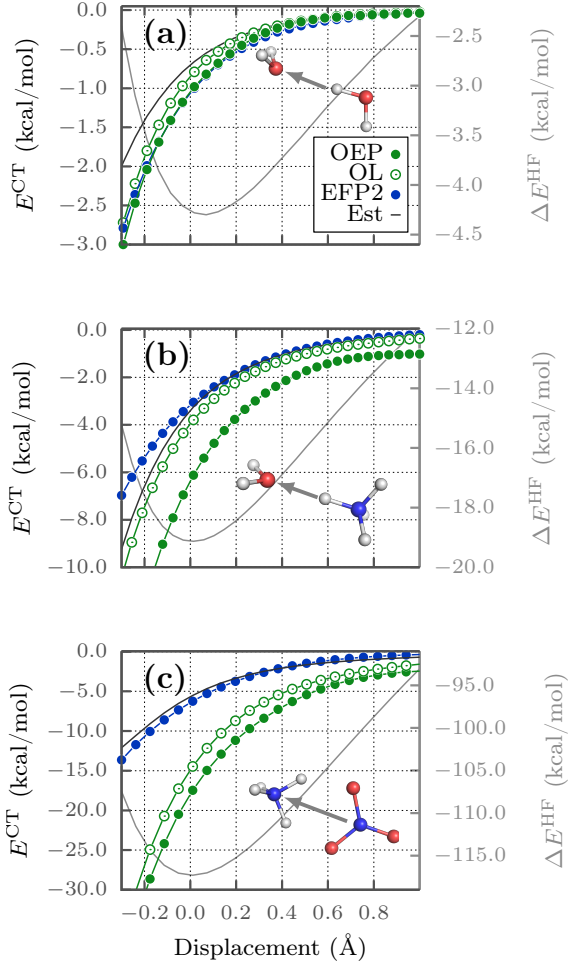


FIG. 1. Asymptotic dependence of the charge transfer energy in the CT/HF0 formulation for selected bi-molecular complexes. (a) water dimer, (b) water-ammonium complex, and (c) ammonium-nitrate complex, were one molecule has been translated along the vector specified in the insets relative to initial geometry, optimized at HF/6-31+G(d,p) level. The total interaction energy is also shown for comparison in light grey color in this figure. Interaction energies were obtained at the HF/6-311++G(2df,2pd) level of theory with the single GDF scheme and aug-cc-pVQZ-jkfit auxiliary basis set.

The asymptotic dependence of the CT energy is shown in Figure 1 and Figure S1 for the methanol-water system. Overall, OEP technique of effective elimination of ERI's sketched in Eq. (13) is sufficiently accurate for water dimer and ammonium nitrate (Figures 1(a) and (c)), and methanol-water system (Figure S1) in all distances studied, reproducing the reference Otto-Ladik CT energy, with errors not exceeding 10% relative to OL es-

timates (compare open and filled green circles). However, in the case of water-ammonium cation complex the OEP method overestimates the CT energy by around 50%, even for large intermonomer separations, where the profile exhibits unphysical long-range tail, visible in Figure 1(b). Careful inspection (see Figure S3) revealed that increasing the size of the auxiliary basis set from aug-cc-pVDZ-jkfit to aug-cc-pVQZ-jkfit slightly improves the performance of the OEP method, however the long-range tail is still appreciable in magnitude even in the aug-cc-pVQZ-jkfit auxiliary basis.

At the moment, it is unclear what causes these errors at large separations. The LOA in  $G_2$  and  $G_3$  may be too drastic approximations when one of the monomers is charged, and more accurate DMTP expansion for the effective densities could be required, also including dipole and higher multipole moments. Interestingly in the case of ammonium nitrate (Figure 1(c)), the relative errors between OEP and OL estimates are not grater than 9% even though both of the monomers are charged. On the other hand, OL method itself strongly overestimates the CT/HF0 energies in this system. Therefore, among the four model complexes, EFP2 and OEP energies coincide with the CT/HF0 estimates only in the case of water dimer and methanol-water complex, in contrast to the EFP2 model, which gives very good estimates of the CT/HF0 energy in mostly all cases at all separations.

Analysis of the statistical sets of dimeric complexes shown in Figures 2(a) and Figures 3(a) suggests that, at least in the case of neutral systems, ERI elimination technique (compare OL and OEP) is of acceptable accuracy with the  $R^2$  coefficients being 74% for the NCB31, and 62% for the BBI dataset. The absolute accuracy of the OEP model, measured with respect to the benchmark CH/HF0 estimates, is shown in Figures 2(b) and Figures 3(b) and the root mean square errors (RMSE) are listed in Table II. In NCB31 set OEP performs better than EFP2 with RMSE of 1.69 and 2.39 kcal/mol, respectively. This is especially the case for charge-transfer-dominated systems (subset CT7/04), in which EFP2 erroneously predict vanishing or even small positive CT energiers (RMSE 4.06), in contrast to OEP method that gives correct signs in all cases and good correlation with the benchmark. On the other hand, EFP2 method very accurately reproduces the CT/HF0 energies in the BBI set ( $R^2 = 95\%$ ) whereas OEP model tends to significantly overestimate the values by a factor of 1.55 with RMSE of 0.56 kcal/mol, unlike the OL model which is more accurate (RMSE of 0.22 and  $R^2 = 78\%$ ).

Since the nature of the EFP2 and OEP models is highly approximate, and the most important goal is to construct efficient and reasonably accurate *ab initio* force field, one can use the fact that OEP model almost always overestimates the CT/HF0 energies with rather good linear correlation, unlike EFP2 model, which can also strongly underestimate it. Therefore, the simple semi-empirical scaling model is proposed here for the OEP-based esti-

TABLE II. Accuracy of approximate CT/HF0 energy methods across wide range of bi-molecular complexes<sup>a</sup>

Database		RMSE (kcal/mol)			
		OL <sup>b</sup>	OEP <sup>c</sup>	EFP2 <sup>d</sup>	
NCB31 <sup>e</sup>	HB6/04	1.38	1.36	0.37	2.45
	DI6/04	0.35	0.66	0.22	0.44
	CT7/04	0.98	2.82	0.71	4.06
	WI7/04	0.01	0.09	0.05	0.02
	PPS5/05	0.07	1.31	0.79	0.60
	Total	0.83	1.69	0.53	2.39
BBI <sup>f</sup>	Total	0.26	0.56	0.13	0.12

<sup>a</sup> Validated against Eq. (65).

<sup>b</sup> Otto and Ladik's expression from Eq. (4) in Ref.<sup>5</sup>

<sup>c</sup> This work, Eq. (71) with  $C = 1.00$  (left column) and  $C = 1.56$  (right column). GDF(1)/aug-cc-pVDZ-jkfit scheme was used for the extended density fitting of group (i) OEP's.

<sup>d</sup> Ref.<sup>22</sup>, Eq. (33).

<sup>e</sup> Ref.<sup>70–72</sup>

<sup>f</sup> Ref.<sup>73</sup>

mate, i.e.,

$$E_{\text{scaled}}^{\text{CT}} \approx C \times E_{\text{unscaled}}^{\text{CT}} \quad (71)$$

where  $C$  is an empirical constant and  $E_{\text{unscaled}}^{\text{CT}}$  is given by Eqs. (32) and Eq. (64). Based on OEP performance from NCB31 and BBI sets, it was estimated that  $C \approx 1.56$ . Application of the semi-empirical model from Eq. (71) significantly improved absolute accuracy of the model in all datasets. For instance, RMSE was reduced down to 0.13 kcal/mol in the BBI set, comparable to EFP2 model. Naturally, the accuracy of the OL model limits the absolute accuracy of the OEP model, which is manifested in the ammonium nitrate system in Figure 1(c) or the problems with LOA. In order to improve the performance for ionic systems, further studies are necessary, that will modify the original formulation of OL and LOA treatment, or use different sets of virtual orbitals<sup>23</sup>. Nevertheless, except from the ionic systems, it is clear that the level of accuracy of the EFP2 and OEP models are rather comparable, especially after applying the empirical scaling, across a wide range of various interacting complexes including systems with H-bonding, dominated by dipole-dipole or dispersion interactions or exhibiting substantial CT.

## B. Reduction of computational costs

The utmost goal of this work is to reduce the computational cost of the CT/HF0 energy evaluation in the calculations involving effective fragment potentials, no longer making it the bottleneck of the EFP2-based interaction

TABLE III. Estimated computational cost of the EFP2 and OEP methods for calculation of CT/HF0 energy<sup>a</sup>

Method	EFP2	OEP
Constant parameters <sup>b</sup>	$\varepsilon_i$	$\varepsilon_i, \varepsilon_n, L_{ii}^A$
Superimposable parameters <sup>b</sup>	$C_{\alpha i}^A, C_{\beta n}^B, \{\alpha\}, \{\beta\}$	$C_{\alpha i}^A, C_{\alpha n}^B, \{\alpha\}, \{\beta\}, \{\eta\}, V_{n\eta}^{\text{eff}, B}$
Calculables <sup>b</sup>	$T_{nn}, T_{kj}, T_{wj}, T_{nj}, U_{in}^{\text{EF}, B}, U_{ik}^{\text{EF}, B}, U_{iw}^{\text{EF}, B}$	$S_{ij}, S_{nk}, S_{nw}, u_i^{BA}, w_{yi}^{BA}$
Cost <sup>c</sup>	$sp(2p^2 + 2op + o^2)$ $+tp(2p^2 + 2op + o^2)$ $+vop(3p + o)$	$sop(2p + o + a)$ $+op(a + oN + 2o)$ $+o^2p$

<sup>a</sup> Based on coupling constant expressions from Eq. (34) and Eq. (63) for EFP2 and OEP method, respectively.

<sup>b</sup> The subscript meaning is as follows: primary basis set functions of  $A$ :  $\alpha$ ; primary basis set functions of  $B$ :  $\beta$ ; auxiliary basis set functions of  $B$ :  $\eta$ ; occupied MO's of  $A$ :  $i, i', k$ ; occupied MO's of  $B$ :  $j$ ; virtual MO's of  $A$ :  $w$ ; virtual MO's of  $B$ :  $n$ ; atoms of  $B$ :  $y$ . Analysis is based on  $E^{A \rightarrow B}$  term.

<sup>c</sup> Numbers of: primary basis set functions -  $p$ ; auxiliary basis set functions -  $a$ ; occupied MO's -  $o$ ; atoms -  $N$ . Relative costs:  $v$  - multipole potential,  $t$  - kinetic energy and  $s$  - overlap OEI's. It was assumed that the number of virtual orbitals is equal to  $n$ .

energy calculations. In Table III estimation of the computational cost of the EFP2 and OEP models is shown. It is apparent that EFP2 requires much more quantities to be computed as compared to the OEP method ('Calculables' in the table). Clearly, evaluation of the EFP2 CT expression from Eq. (33) involves quite a number of different types of OEI's. According to our estimations that assume sequential (two-step) two-index AO-MO transformations of OEI matrices and large AO basis sets, the computational cost is of an order of  $2p^3(s + t) + 3vop^2$ , where the  $o$  and  $p$  denote the number of occupied orbitals and the number of atomic basis functions, respectively. Here,  $s, t$  and  $v$  are the relative costs of evaluation of the overlap, kinetic energy, and multipole potential OEI's, respectively, with the latter being most expensive but necessary to compute  $\mathbf{U}^{\text{EF}}$  matrices from Eq. (36). On the contrary, OEP-based expression from Eq. (64) requires only overlap OEI's that are the least expensive, and has the cost of approximate magnitude of  $2sop^2$  for relatively small auxiliary basis sets. Note also that, among the calculables that are needed in each OEP-based CT energy evaluation, are the auxiliary vectors and matrices from Eqs. (61a) and (61b), the cost of which is negligible. The amount of effective fragment parameters, that needs to be superimposed during the calculations by applying rotation of orbitals and basis functions ('Superimposable parameters') is rather the same in EFP2 and OEP models. This includes the LCAO-MO coefficients in canonical

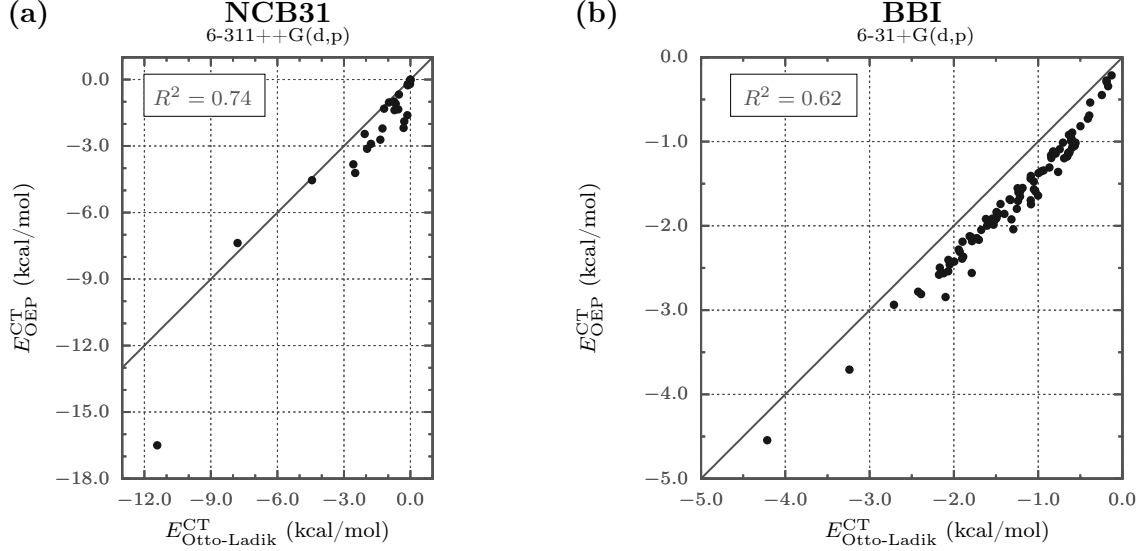


FIG. 2. **Accuracy of the ERI elimination technique.** (a) NCB31 database,<sup>70–72</sup> and (b) BBI subset<sup>73</sup> from the BioFragment Database. For the OEP calculations, the EDF-1 scheme with the aug-cc-pVDZ-jkfit auxiliary basis set was used.

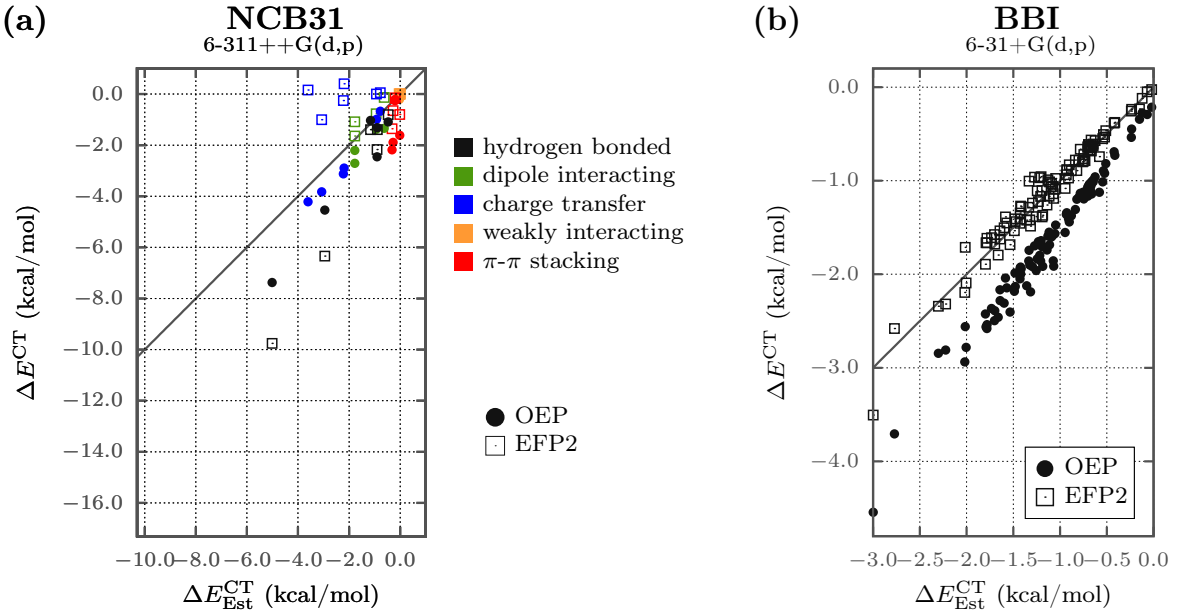


FIG. 3. **Performance of the OEP and EFP2 methods for the CT/HF0 charge transfer interaction energy in bi-molecular neutral complexes.** (a) NCB31 set from database developed by the Truhlar's group<sup>70–72</sup>; the HB6/04 hydrogen bonding database (black),<sup>70–72</sup> the DI6/04 dipole interaction database (green),<sup>70–72</sup> the CT7/04 charge-transfer complex database (blue),<sup>70–72</sup> the WI7/05 weak interaction database (yellow),<sup>70,72,75</sup> and the PPS5/05 the  $\pi$ - $\pi$  stacking database (red);<sup>70,72,75</sup> (b) BBI subset<sup>73</sup> from the BioFragment Database. The EDF-1 scheme with the aug-cc-pVDZ-jkfit auxiliary basis set for the OEP calculations.

TABLE IV. Minimal uncontracted auxiliary basis set optimized for OEP-based CT/HF0 calculations<sup>a</sup>

AO's		Exponents (a.u.)	
		Methanol	Water
H	1s	7.7369294534	29.5837988322
C	1s	880.3654511045	
	2s	123.8276940826	
	2p	11.6748155072	
O	1s	902.9798919021	1030.5721050297
	2s	203.7584408153	142.1022267153
	2p	20.2442429692	40.9175702474

<sup>a</sup> Fitting performed according to Appendix (A) assuming 6-311++G(d,p) and aug-cc-pVDZ-jkfit primary and test basis sets, respectively.

basis, and the primary basis set, with an addition of the auxiliary basis set for the OEP model. Therefore, the cost of parameter superimposition should not be significantly larger as in the EFP2 formulation, provided sufficiently small auxiliary basis set is used. For example, assuming a water dimer system and 6-311++G(d,p) primary and minimal auxiliary basis set with  $s = t = v \approx 1$ , the OEP method is predicted to be roughly 12–16 times faster than EFP2 method. In practice, the parameters  $s$ ,  $t$  and  $v$  will have larger values, especially  $v$ .

TABLE V. CPU timings in milliseconds of CT/HF0 single point energy calculations for water-methanol complex at 6-311++G(d,p) primary basis set<sup>a</sup>

	Water-Methanol	Water dimer
OL	$1.48 \times 10^4$ (-0.81)	$2.91 \times 10^3$ (-0.85)
EFP2	42.7 (-1.27)	15.6 (-1.06)
OEP/aug-cc-pVQZ-jkfit	4.36 (-1.03)	1.64 (-1.05)
OEP/aug-cc-pVTZ-jkfit	3.63 (-1.07)	1.35 (-1.09)
OEP/aug-cc-pVDZ-jkfit	3.60 (-1.05)	1.26 (-1.03)
OEP/6-311++G(d,p)	2.74 (-1.37)	0.933 (-1.31)
OEP/mini <sup>b</sup>	2.25 (-1.34)	0.623 (-1.13)

<sup>a</sup> 1.2 GHz AMD EPYC<sup>TM</sup> 7301 16-Core Processor, calculations performed on 1 core. CT/HF0 energies are given in parentheses for reference (kcal/mol). See also the implementation details in Section IV and Section VB.

<sup>b</sup> This work, Table IV.

In this work, the minimal uncontracted auxiliary basis sets were optimized for water and methanol that consist of only  $s$  and  $p$ -type functions, and the orbital exponents are shown in Table IV whereas the procedure is outlined in Appendix A. Unfortunately, we were not able to successfully fit the auxiliary basis sets for  $\text{NH}_4^+$  and  $\text{NO}_3^-$  using current approach and the basis set opti-

mization falls out of scope of this work. Nevertheless, we found that in the case of neutral systems minimal basis sets are already sufficient to reach required accuracy. In Figure 4 the asymptotic dependence of the CT/HF0 energy for water-methanol system is correctly reproduced by the OEP/mini variant which performs comparably well as the OEP/aug-cc-pVQZ-jkfit. The total time required for evaluation of the CT/HF0 energies by using EFP2 and OEP models was measured for this system and also for the water-water system in their reference geometries, and the results are shown in Table V. Time profiling of the code for OL, EFP2 and OEP methods was performed for all the computational operations required for a single point calculation in a hypothetical sequential run on multiple geometries. Therefore, calculations of intermonomer ERI's in AO basis along with their four-index transformation to MO basis were included in time profiling of the OL routine in our computer code. For the EFP2 and OEP methods, all the calculables were taken into account in the profiling, i.e., calculations of OEI's in AO basis and their two-index transformations to MO basis. Calculations of canonical orbital energies and LCAO-MO coefficients through the self-consistent field HF procedure, as well as calculations of the OEP matrices from Eq. (41) via EDF-2 scheme and atomic effective charges from Eq. (B1a) using the OED in Eq. (56) were not included because these quantities constitute the effective fragments by definition. The above time profiling setting allows one to compare the performances of the OL, EFP2 and OEP methods as effective fragment parameter methods.

Even for the rather large quadruple- $\zeta$  auxiliary basis set, the OEP-based model is roughly 10 times more efficient than evaluating the EFP2 CT energy. Reducing the size of auxiliary basis set up to minimal basis from Table IV scales down the cost further by a factor of 2.0 in water-methanol system, and 2.6 in water dimer system, reaching in total roughly 20-fold reduction in CPU time as compared to the EFP2 model, and more than three orders of magnitude as compared to the OL model. Since the size of such a minimal basis is very small when compared to the primary basis sets recommended for constructing the EFP2 parameters, the additional superimposition costs of the auxiliary basis should be negligible. It is also worth mentioning here that, while using the usual 6-311++G(d,p) basis in a role of auxiliary basis set gave already accurate results, the minimal STO-3G basis as auxiliary space resulted in CT energies of -8.4 and -8.8 kcal/mol in water-methanol and water dimer systems (data not shown), much lower than the reference values of -0.81 and -0.85 kcal/mol, respectively. Therefore, the basis set optimization described in Appendix A was necessary for the minimal basis to be applicable in the CT calculations using OEP technique, with OEP's generated by the EDF-2 scheme developed in Section II C 2.

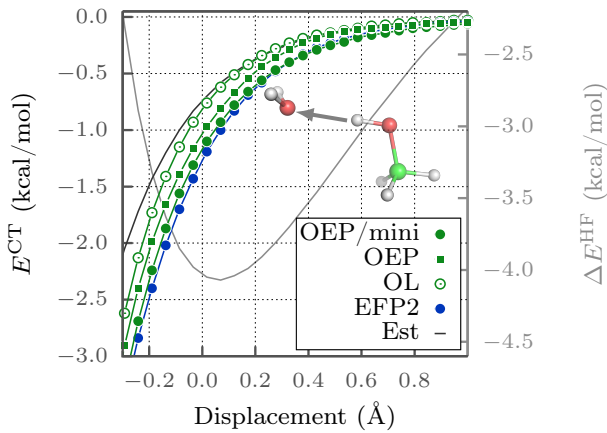


FIG. 4. Asymptotic dependence of the charge transfer energy in the CT/HF0 formulation for methanol-water complex with minimal OEP auxiliary basis. Water molecule has been translated by  $R$  from the starting geometry optimized at HF/6-31+G(d,p) level, along the vector specified in the insets. The total interaction energy is also shown for comparison in light grey color in this figure. Interaction energies were obtained at the HF/6-31++G(d,p) level of theory. In this figure, ‘OEP’ denotes single GDF scheme with aug-cc-pVQZ-jkfit auxiliary basis set whereas ‘OEP/mini’ denotes double GDF scheme with the minimal auxiliary basis given in Table IV.

## VI. SUMMARY AND A FEW CONCLUDING REMARKS

In this work, the one-electron effective potential operator technique of eliminating electron repulsion integrals in the fragment-based theories of intermolecular interactions was proposed. It was shown that in general case two types of OEP’s can be defined and worked out either through the density fitting or the distributed multipole expansion. For the first group of OEP’s, the density fitting was extended and two computational treatments of OEP’s were developed: the EDF-1 scheme for RI-type auxiliary basis sets, as well as the EDF-2 scheme, for essentially all other types of basis sets. The OEP technique was then applied to calculating the charge transfer energy in condensed phases simulations. The presented validation of the OEP technique against the Otto-Ladik CT/HF0 model as parent theory showed that in most cases elimination of ERI’s is quantitatively accurate, with few exceptions where only qualitative accuracy was found. Finally, it was concluded that, while the proposed OEP-based Otto-Ladik model is of comparable accuracy as the CT/HF0 formulation within the state-of-the-art EFP2 model, it significantly outperforms the latter in terms of computational efficiency reaching speedups up to 20 times. It should be emphasized that there is still more room for optimization of the OEP technique. First of all, not only group (i) terms, but also all the summations over the virtual orbitals can be optimized, e.g., by using the QUAMBO’s, following Xu and

Gordon.<sup>23</sup> Secondly, effective atomic charges  $q_y^{B,(nj)}$  from Eq. (58) are most of the time very small and could be neglected, leading to further cost reductions (not shown here). In addition, the possibility of the OEP-based formulation of the direct EFP2 CT formulation should be studied in the future as well. Therefore, it is believed that the OEP-based model can be incorporated within the EFP2 method, strongly facilitating the full (CT-including) EFP2 energy calculations and molecular dynamics simulations in large systems. However, the current model needs to be improved by further investigating the ionic systems in detail and possibly revising the LOA and EDF approximations. Nevertheless, it is anticipated here that the OEP method of ERI elimination can be used in virtually any other *ab initio* fragment-based approaches for condensed-phase simulations, where ERI’s pose the computational challenge when confronted with the size of the system.

## ACKNOWLEDGMENTS

This project is carried out under POLONEZ programme which has received funding from the European Union’s Horizon 2020 research and innovation programme under the Marie Skłodowska-Curie grant agreement No. 665778. This project is funded by National Science Centre, Poland (grant no. 2016/23/P/ST4/01720) within the POLONEZ 3 fellowship. Wroclaw Centre for Networking and Supercomputing (WCSS) is acknowledged for computational resources. We cordially thank Professor Marcos Mandado from University of Vigo in Spain for providing us with his benchmark calculations to validate our implementation of the DDS method.

## Appendix A: Optimized Auxiliary Basis Sets for OEP Applications

To fit the auxiliary DF basis for the treatment of the overlap-like OEP matrix elements with the operator  $\hat{v}_{\text{eff}}$ , the following objective function is minimized

$$Z[\{\xi\}] = \sum_{\alpha i} \left[ \langle \alpha | \hat{v}_{\text{eff}} | i \rangle - \sum_{\xi}^{\text{DF}} V_{\xi i} S_{\alpha \xi} \right]^2, \quad (\text{A1})$$

where  $\{\xi\}$  is the auxiliary basis set to optimize, whereas  $\{\alpha\}$  is the ‘test’ basis set used to probe the accuracy of the density fitting. The forms of the charge-transfer DF matrices  $\langle \alpha | \hat{v}_{\text{eff}} | i \rangle$  can be directly derived from Eq. (41) by expanding the MO’s in terms of the AO’s. The working formula is

$$\langle \alpha | \hat{v}_{\text{eff}}^{G_1} | n \rangle = - \sum_x^{\text{At}} W_{\alpha n}^{(x)} + \sum_{\beta \gamma \delta} \{2C_{\beta n} D_{\gamma \delta} - C_{\gamma n} D_{\beta \delta}\} \langle \alpha \beta | \gamma \delta \rangle \quad (\text{A2})$$

for the OEP operator defined by

$$\sum_{\eta \in B}^{\text{DF}} \hat{v}_{\text{eff}}^{\text{G}_1} |\eta\rangle \equiv \sum_{\eta \in B}^{\text{DF}} V_{n\eta}^B |\eta\rangle. \quad (\text{A3})$$

In Eq. (A2),  $\mathbf{C}$  is the LCAO-MO matrix whereas  $\mathbf{D}$  is the one-particle density matrix in AO basis.

## Appendix B: Coulomb-like OEP via Cumulative Atomic Multipole Moments

Overlap-like OEP's are always associated with the effective one-particle density (or bond-order) matrices and the  $\lambda$  parameter from Eq. (5) being either 1 or 0. Therefore, one can use this fact to compute the effective distributed multipole moments. In this work, the cumulative atomic multipole moments (CAMM) of Sokalski and Poirier with Mulliken partitioning of the AO space were chosen because of their simplicity. One of examples of such OEP-based models reported already in the literature is the transition cumulative atomic multipole moments (TrCAMM) model for estimation of the excitation energy transfer (EET) couplings in the Förster limit<sup>61</sup>, or the vibrational solvatochromic distributed multipole moments (SolCAMM) for the determination of the vibrational frequency shifts of spatially localized IR probes.<sup>60</sup> In general, having the OED and  $\lambda$ , the effective cumulative atomic charges and dipole moments are given by

$$q_x^{\text{eff}} = \lambda Z_x - \sum_{\alpha \in x} \sum_{\beta} P_{\alpha\beta}^{\text{eff}} \langle \alpha | \beta \rangle, \quad (\text{B1a})$$

$$\mu_x^{\text{eff}} = \sum_{\alpha \in x} \sum_{\beta} P_{\alpha\beta}^{\text{eff}} \{ \langle \alpha | \beta \rangle \mathbf{R}_x - \langle \alpha | \hat{\mathbf{r}} | \beta \rangle \}, \quad (\text{B1b})$$

where  $\mathbf{R}_x$  is the position vector of the  $x$ -th nucleus. Note that  $P_{\alpha\beta}^{\text{eff}}$  can refer to the particular electron spin, or their sum as a bond order matrix as well. Equations for the effective distributed quadrupoles, octupoles and hexadecapoles can be easily obtained by analogy from Ref.<sup>61</sup>

- <sup>1</sup>P. Otto and J. Ladik, *Int. J. Quant. Chem.* **18**, 1143 (1980).
- <sup>2</sup>A. J. Stone, *The Theory of Intermolecular Forces*, (Clarendon Press, Oxford, 1996).
- <sup>3</sup>C. C. J. Roothaan, *Rev. Mod. Phys.* **23**, 69 (1951).
- <sup>4</sup>J. H. Jensen, *J. Chem. Phys.* **114**, 8775 (2001).
- <sup>5</sup>P. Otto and J. Ladik, *Chem. Phys.* **8**, 192 (1975).
- <sup>6</sup>B. Jeziorski, R. Moszyński, and K. Szalewicz, *Chem. Rev.* **94**, 1887 (1994).
- <sup>7</sup>A. J. Stone and A. J. Misquitta, *Chem. Phys. Lett.* **473**, 201 (2009).
- <sup>8</sup>J. N. Murrell, M. Randić, D. R. Williams, and H. C. Longuet-Higgins, *Proc. R. Soc. Lond. A* **284**, 566 (1965).
- <sup>9</sup>M. S. Gordon, D. G. Fedorov, S. R. Pruitt, and L. V. Slipchenko, *Chem. Rev.* **112**, 632 (2012).
- <sup>10</sup>O. Demerdash, Y. Mao, T. Liu, M. Head-Gordon, and T. Head-Gordon, *J. Chem. Phys.* **147**, 161721 (2017).
- <sup>11</sup>W. Sokalski and R. Poirier, *Chem. Phys. Lett.* **98**, 86 (1983).
- <sup>12</sup>C. Etchebest, R. Lavery, and A. Pullman, *Theor. Chem. Acc.* **62**, 17 (1982).
- <sup>13</sup>A. J. Stone, *J. Chem. Theory Comput.* **1**, 1128 (2005).

- <sup>14</sup>O. Demerdash, E.-H. Yap, and T. Head-Gordon, *Annu. Rev. Phys. Chem.* **65**, 149 (2014).
- <sup>15</sup>P. Xu, E. B. Guidez, C. Bertoni, and M. S. Gordon, *J. Chem. Phys.* **148**, 090901 (2018).
- <sup>16</sup>M. S. Gordon, Q. A. Smith, P. Xu, and L. V. Slipchenko, *Annu. Rev. Phys. Chem.* **64**, 553 (2013).
- <sup>17</sup>K. A. Nguyen, R. Pachter, and P. N. Day, *J. Chem. Phys.* **140**, 244101 (2014).
- <sup>18</sup>P. N. Day, J. H. Jensen, M. S. Gordon, S. P. Webb, W. J. Stevens, M. Krauss, D. Garmer, H. Basch, and D. Cohen, *J. Chem. Phys.* **105**, 1968 (1996).
- <sup>19</sup>T. Sattasathuchana, P. Xu, and M. S. Gordon, *J. Phys. Chem. A* **123**, 8460 (2019).
- <sup>20</sup>N. Kuroki and H. Mori, *Chem. Lett.* **45**, 1009 (2016).
- <sup>21</sup>M. K. Ghosh, S. G. Cho, and C. H. Choi, *J. Phys. Chem. B* **118**, 4876 (2014).
- <sup>22</sup>H. Li, M. S. Gordon, and J. H. Jensen, *J. Chem. Phys.* **124**, 214108 (2006).
- <sup>23</sup>P. Xu and M. S. Gordon, *J. Chem. Phys.* **139**, 194104 (2013).
- <sup>24</sup>N. Gresh, P. Claverie, and A. Pullman, *Theoret. Chim. Acta* **66**, 1 (1984).
- <sup>25</sup>J.-P. Piquemal, H. Chevreau, and N. Gresh, *J. Chem. Theory Comput.* **3**, 824 (2007).
- <sup>26</sup>H. R. Leverentz, K. A. Maerzke, S. J. Keasler, J. I. Siepmann, and D. G. Truhlar, *Phys. Chem. Chem. Phys.* **14**, 7669 (2012).
- <sup>27</sup>E. E. Dahlke and D. G. Truhlar, *J. Chem. Theory Comput.* **4**, 1 (2008).
- <sup>28</sup>J. H. Jensen and M. S. Gordon, *Mol. Phys.* **89**, 1313 (1996).
- <sup>29</sup>J. H. Jensen and M. S. Gordon, *J. Chem. Phys.* **108**, 4772 (1998).
- <sup>30</sup>H. Li, H. M. Netzloff, and M. S. Gordon, *J. Chem. Phys.* **125**, 194103 (2006).
- <sup>31</sup>I. Adamovic and M. S. Gordon, *Mol. Phys.* **103**, 379 (2005).
- <sup>32</sup>P. Xu, F. Zahariev, and M. S. Gordon, *J. Chem. Theory Comput.* **10**, 1576 (2014).
- <sup>33</sup>L. V. Slipchenko and M. S. Gordon, *J. Comput. Chem.* **28**, 276 (2007).
- <sup>34</sup>G. Chałasiński and M. Gutowski, *Mol. Phys.* **54**, 1173 (1985).
- <sup>35</sup>B. Blasiak, C. H. Londergan, L. J. Webb, and M. Cho, *Acc. Chem. Res.* **50**, 968 (2017).
- <sup>36</sup>B. Blasiak, A. W. Ritchie, L. J. Webb, and M. Cho, *Phys. Chem. Chem. Phys.* **18**, 18094 (2016).
- <sup>37</sup>R. J. Xu, B. Blasiak, M. Cho, J. P. Layfield, and C. H. Londergan, *J. Phys. Chem. Lett.* **9**, 2560 (2018).
- <sup>38</sup>P. K. Gurunathan, A. Acharya, D. Ghosh, D. Kosenkov, I. Kaliman, Y. Shao, A. I. Krylov, and L. V. Slipchenko, *J. Phys. Chem. B* **120**, 6562 (2016).
- <sup>39</sup>D. Ghosh, D. Kosenkov, V. Vanovschi, C. F. Williams, J. M. Herbert, M. S. Gordon, M. W. Schmidt, L. V. Slipchenko, and A. I. Krylov, *J. Phys. Chem. A* **114**, 12739 (2010).
- <sup>40</sup>C. Møller and M. S. Plesset, *Phys. Rev.* **46**, 618 (1934).
- <sup>41</sup>M. W. Schmidt, K. K. Baldridge, J. A. Boatz, S. T. Elbert, M. S. Gordon, J. H. Jensen, S. Koseki, N. Matsunaga, K. A. Nguyen, S. Su, T. L. Windus, M. Dupuis, and J. A. Montgomery, *J. Chem. Phys.* **14**, 1347 (1993).
- <sup>42</sup>W. C. Lu, C. Z. Wang, M. W. Schmidt, L. Bytautas, K. M. Ho, and K. Ruedenberg, *J. Chem. Phys.* **120**, 2629 (2004).
- <sup>43</sup>N. Kuroki and H. Mori, *J. Phys. Chem. B* **123**, 194 (2019).
- <sup>44</sup>T. Giovannini, P. Lafiosca, and C. Cappelli, *J. Chem. Theory Comput.* **13**, 4854 (2017).
- <sup>45</sup>S. Budzák, A. D. Laurent, C. Laurence, M. Medved, and D. Jacquemin, *J. Chem. Theory Comput.* **12**, 1919 (2016).
- <sup>46</sup>Q. A. Smith, M. S. Gordon, and L. V. Slipchenko, *J. Phys. Chem. A* **115**, 11269 (2011).
- <sup>47</sup>Q. A. Smith, M. S. Gordon, and L. V. Slipchenko, *J. Phys. Chem. A* **115**, 4598 (2011).
- <sup>48</sup>T. Smith, L. V. Slipchenko, and M. S. Gordon, *J. Phys. Chem. A* **112**, 5286 (2008).
- <sup>49</sup>I. A. Kaliman and L. V. Slipchenko, *J. Comput. Chem.* **36**, 129 (2015).

<sup>50</sup>D. Ghosh, D. Kosenkov, V. Vanovschi, J. Flick, I. Kaliman, Y. Shao, A. T. Gilbert, A. I. Krylov, and L. V. Slipchenko, *J. Comput. Chem.* **34**, 1060 (2013).

<sup>51</sup>A. Devarajan, A. Gaenko, M. S. Gordon, and T. L. Windus, “Nucleation using the effective fragment potential and two-level parallelism,” in *Fragmentation* (John Wiley Sons, Ltd, 2017) Chap. 7, pp. 209–226.

<sup>52</sup>A. Devarajan, T. L. Windus, and M. S. Gordon, *J. Phys. Chem. A* **115**, 13987 (2011).

<sup>53</sup>P. Hohenberg and W. Kohn, *Phys. Rev.* **136**, B864 (1964).

<sup>54</sup>W. Kohn and L. J. Sham, *Phys. Rev.* **140**, A1133 (1965).

<sup>55</sup>A. Holas and N. H. March, *Phys. Rev. A* **44**, 5521 (1991).

<sup>56</sup>W. Weber and W. Thiel, *Theor. Chem. Acc.* **103**, 495 (2000).

<sup>57</sup>F. Neese, *J. Chem. Phys.* **122**, 034107 (2005).

<sup>58</sup>G. A. Cisneros, J.-P. Piquemal, and T. A. Darden, *J. Chem. Phys.* **123**, 044109 (2005).

<sup>59</sup>J.-P. Piquemal, G. A. Cisneros, P. Reinhardt, N. Gresh, and T. A. Darden, *J. Chem. Phys.* **124**, 104101 (2006).

<sup>60</sup>B. Blasiak, H. Lee, and M. Cho, *J. Chem. Phys.* **139**, 044111 (2013).

<sup>61</sup>B. Blasiak, M. Maj, M. Cho, and R. W. Góra, *J. Chem. Theory Comput.* **11**, 3259 (2015).

<sup>62</sup>B. Blasiak and M. Cho, *J. Chem. Phys.* **140**, 164107 (2014).

<sup>63</sup>A. Stone and M. Alderton, *Mol. Phys.* **56**, 1047 (1985).

<sup>64</sup>C. M. Breneman and K. B. Wiberg, *J. Comput. Chem.* **11**, 361 (1990).

<sup>65</sup>A. Heßelmann, G. Jansen, and M. Schütz, *J. Chem. Phys.* **122**, 014103 (2005).

<sup>66</sup>L. E. McMurchie and E. R. Davidson, *J. Comput. Phys.* **26**, 218 (1978).

<sup>67</sup>G. M. J. Barca and P.-F. Loos, *J. Chem. Phys.* **147**, 024103 (2017).

<sup>68</sup>W. J. Stevens and W. H. Fink, *Chem. Phys. Lett.* **139**, 15 (1987).

<sup>69</sup>M. J. Frisch, G. W. Trucks, H. B. Schlegel, G. E. Scuseria, M. A. Robb, J. R. Cheeseman, G. Scalmani, V. Barone, G. A. Petersson, H. Nakatsuji, X. Li, M. Caricato, A. V. Marenich, J. Bloino, B. G. Janesko, R. Gomperts, B. Mennucci, H. P. Hratchian, J. V. Ortiz, A. F. Izmaylov, J. L. Sonnenberg, D. Williams-Young, F. Ding, F. Lipparini, F. Egidi, J. Goings, B. Peng, A. Petrone, T. Henderson, D. Ranasinghe, V. G. Zakrzewski, J. Gao, N. Rega, G. Zheng, W. Liang, M. Hada, M. Ehara, K. Toyota, R. Fukuda, J. Hasegawa, M. Ishida, T. Nakajima, Y. Honda, O. Kitao, H. Nakai, T. Vreven, K. Throssell, J. A. Montgomery, Jr., J. E. Peralta, F. Ogliaro, M. J. Bearpark, J. J. Heyd, E. N. Brothers, K. N. Kudin, V. N. Staroverov, T. A. Keith, R. Kobayashi, J. Normand, K. Raghavachari, A. P. Rendell, J. C. Burant, S. S. Iyengar, J. Tomasi, M. Cossi, J. M. Millam, M. Klene, C. Adamo, R. Cammi, J. W. Ochterski, R. L. Martin, K. Morokuma, O. Farkas, J. B. Foresman, and D. J. Fox, “Gaussian 16 Revision C.01,” (2016), Gaussian Inc. Wallingford CT.

<sup>70</sup>Y. Zhao, N. E. Schultz, and D. G. Truhlar, *J. Chem. Theory Comput.* **2**, 364 (2006).

<sup>71</sup>Y. Zhao and D. G. Truhlar, *J. Chem. Theory Comput.* **1**, 415 (2005).

<sup>72</sup>Y. Zhao, N. E. Schultz, and D. G. Truhlar, *J. Chem. Phys.* **123**, 161103 (2005).

<sup>73</sup>L. A. Burns, J. C. Faver, Z. Zheng, M. S. Marshall, D. G. A. Smith, K. Vanommeslaeghe, A. D. MacKerell, K. M. Merz, and C. D. Sherrill, *J. Chem. Phys.* **147**, 161727 (2017).

<sup>74</sup>R. M. Parrish, L. A. Burns, D. G. A. Smith, A. C. Simmonett, A. E. DePrince, III, E. G. Hohenstein, U. Bozkaya, A. Y. Sokolov, R. Di Remigio, R. M. Richard, J. F. Gonthier, A. M. James, H. R. McAlexander, A. Kumar, M. Saitow, X. Wang, B. P. Pritchard, P. Verma, H. F. Schaefer, III, K. Patkowski, R. A. King, E. F. Valeev, F. A. Evangelista, J. M. Turney, T. D. Crawford, and C. D. Sherrill, *J. Chem. Theory Comput.* **13**, 3185 (2017).

<sup>75</sup>Y. Zhao and D. G. Truhlar, *J. Phys. Chem. A* **109**, 5656 (2005).

<sup>76</sup>M. Mandado and J. M. Hermida-Ramón, *J. Chem. Theory Comput.* **7**, 633 (2011).

<sup>77</sup>I. Hayes and A. Stone, *Molecular Physics* **53**, 83 (1984).

<sup>78</sup>R. McWeeny, *Rev. Mod. Phys.* **32**, 335 (1960).

<sup>79</sup>J. L. Dodds, R. McWeeny, and A. J. Sadlej, *Mol. Phys.* **34**, 1779 (1977).

<sup>80</sup>S. F. Boys, *Rev. Mod. Phys.* **32**, 296 (1960).

<sup>81</sup>J. Pipek and P. G. Mezey, *J. Chem. Phys.* **90**, 4916 (1989).

## Supplementary Information

### Ab Initio Effective One-Electron Potential Operators. I. Applications for Charge-Transfer Energy in Effective Fragment Potentials

Bartosz Błasiak,<sup>1, a)</sup> Joanna D. Bednarska,<sup>1</sup> Marta Chołuj,<sup>1</sup> and Wojciech Bartkowiak<sup>1</sup>

*Department of Physical and Quantum Chemistry, Faculty of Chemistry,  
Wrocław University of Science and Technology, Wybrzeże Wyspiańskiego 27,  
Wrocław 50-370, Poland*

(Dated: 4 February 2020)

---

<sup>a)</sup>blasiak.bartosz@gmail.com; <https://www.polonez.pwr.edu.pl>

## CONTENTS

I. Asymptotic dependence of CT interactions for methanol-water complex	2
II. Validation of EFP2 implementation vs GAMESS US	3
III. Auxiliary basis set dependence of CT/HF0 energy	5
References	6

## I. ASYMPTOTIC DEPENDENCE OF CT INTERACTIONS FOR METHANOL-WATER COMPLEX

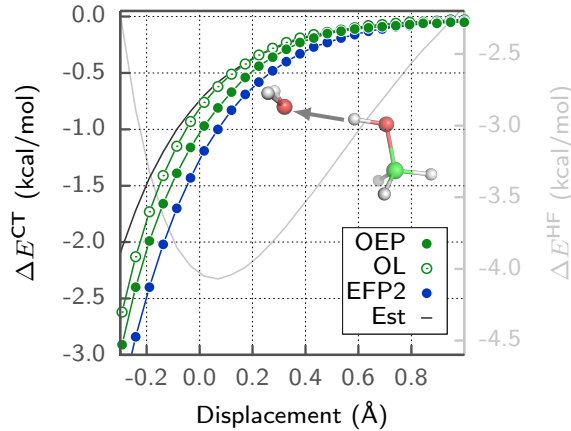


FIG. S1. **Asymptotic dependence of the charge transfer energy in the CT/HF0 formulation for water-methanol complex.** Water molecule has been translated by  $R$  from the starting geometry along the vector specified in the inset picture. The counterpoise-corrected total interaction energy is also shown for comparison in light grey color in this figure. All data were obtained at HF/6-311++G(d,p) level of theory with the EDF-1 scheme and aug-cc-pVQZ-jkfit auxiliary basis set.

## II. VALIDATION OF EFP2 IMPLEMENTATION VS GAMESS US

In Figure S2 interaction energy components obtained by using the code developed in this work are compared to the ones obtained by using the EFP2 calculation routines in GAMESS US quantum chemistry package<sup>1</sup> (version: Sept 30, 2017 R2 Public Release). For this, EFP2 parameters were generated by running the `MAKEFP` routine with `CTVVO` option switched to `.FALSE.` which corresponds to using all the canonical molecular orbitals from HF calculations instead of valence virtual orbitals. Generally, Coulombic energies (Figure S2(a)) are in very good agreement with a few exceptions in the PPS5 set, for which the differences are due to the inaccuracies in the DMTP expansion used in the EFP2 model – note that the Coulombic component in the DDS/HF method is free from multipole approximation and is equivalent to the first-order SAPT Coulombic energy. Exchange-repulsion and induction energies (Figures S2(b) and S2(c), respectively) are in very good agreement. CT energies (Figure S2(d)) evaluated with CAMM up to quadrupoles for the potential energy matrix elements (black filled circles) are generally also in decent quantitative agreement, except for  $\text{NH}_3\text{-FCl}$ ,  $(\text{HCOOH})_2$  and  $(\text{HCONH}_2)_2$  where the differences are between 2–4 kcal/mol. Only in the case of the latter three systems, adding distributed octupoles (blue crosses in Figure S2(d)) lowers the CT energy values by around 1 kcal/mol, with negligible changes for the rest.

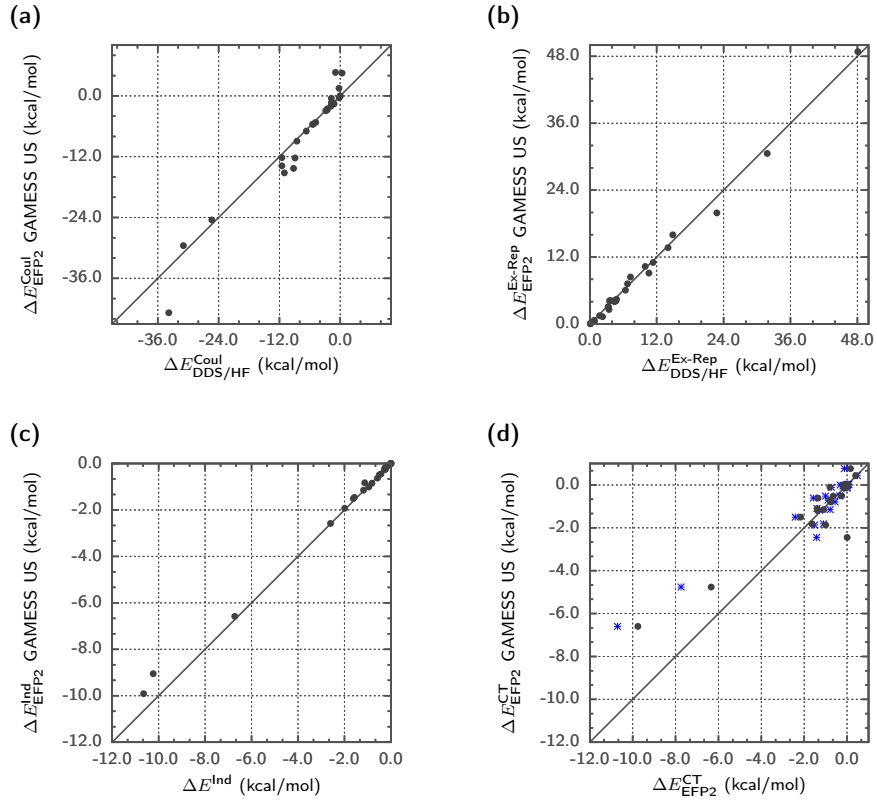


FIG. S2. Validation of implementation of the interaction energy components with respect to the EFP2 GAMESS US code. Results obtained for the NCB31 database set assuming 6-311++G(d,p) primary basis set. (a) - Coulombic, (b) - exchange-repulsion, (c) - induction, and (d) - charge-transfer interaction energy. In (d), black circles and blue crosses correspond to the CT EFP2 energies with CAMM up to distributed quadrupoles and octupoles, respectively. For more details see the main text (Section III, *Calculation Details*).

### III. AUXILIARY BASIS SET DEPENDENCE OF CT/HF0 ENERGY

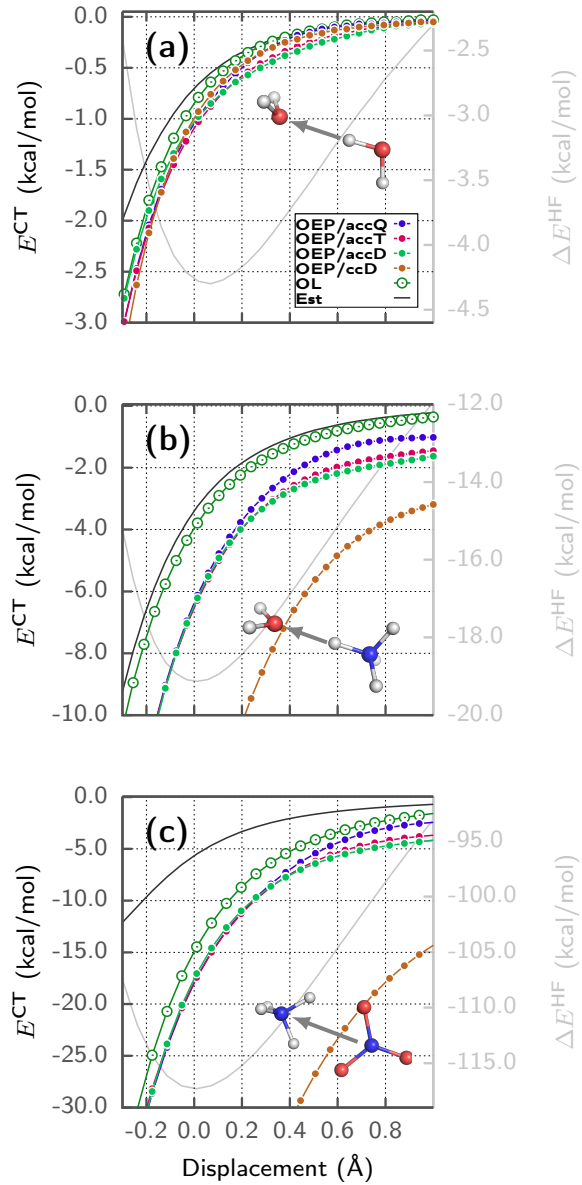


FIG. S3. Effect of auxiliary basis set size on the asymptotic dependence of CT/HF0 energies in model bi-molecular complexes. Auxiliary basis sets were abbreviated for convenience as follows: ccD – cc-pVDZ, accX – aug-cc-pVXZ where X=D,T,Q.

## REFERENCES

<sup>1</sup>M. W. Schmidt, K. K. Baldridge, J. A. Boatz, S. T. Elbert, M. S. Gordon, J. H. Jensen, S. Koseki, N. Matsunaga, K. A. Nguyen, S. Su, T. L. Windus, M. Dupuis, and J. A. Montgomery, *J. Chem. Phys.* **14**, 1347 (1993).